The Effect of Sedimentation And Diagenesis on Trace Element Composition of Water-Laid Tuff in the Keg Mountain Area, Utah

GEOLOGICAL SURVEY PROFESSIONAL PAPER 818-C

The Effect of Sedimentation And Diagenesis on Trace Element Composition of Water-Laid Tuff in the Keg Mountain Area, Utah

By DAVID A. LINDSEY

BERYLLIUM-BEARING TUFFS IN WESTERN UTAH

GEOLOGICAL SURVEY PROFESSIONAL PAPER 818-C

A statistical study of the petrogenesis of unmineralized water-laid tuff in the western Utah beryllium belt

UNITED STATES GOVERNMENT PRINTING OFFICE, WASHINGTON : 1975

UNITED STATES DEPARTMENT OF THE INTERIOR

ROGERS C. B. MORTON, *Secretary*

GEOLOGICAL SURVEY

V. E. McKelvey, *Director*

Library of Congress Cataloging in Publication Data
Lindsey, David A.
The effect of sedimentation and diagenesis on trace element composition of water-laid tuff in the Keg Mountain area, Utah.
(Geological Survey Professional Paper 818–C: Beryllium-bearing tuffs in western Utah)
Bibliography: p.
Supt. of Docs. no.: I 19.16:818–C
1. Volcanic ash, tuff, etc.—Utah—Keg Mountain region. 2. Beryllium ores—Utah—Keg Mountain region. 3. Trace elements.
I. Title. II. Series: United States Geological Survey Professional Paper 818–C. III. Series: Beryllium-bearing tuffs in western Utah.
QE461.L623 552'.2 74-30055

For sale by the Superintendent of Documents, U.S. Government Printing Office
Washington, D.C. 20402
Stock Number 024-001-02661-9

CONTENTS

ILLUSTRATIONS

CONTENTS

TABLES

BERYLLIUM-BEARING TUFFS IN WESTERN UTAH

THE EFFECT OF SEDIMENTATION AND DIAGENESIS ON TRACE ELEMENT COMPOSITION OF WATER-LAID TUFF IN THE KEG MOUNTAIN AREA, UTAH

By DAVID A. LINDSEY

ABSTRACT

The mineral and trace element composition of water-laid tuff in the Keg Mountain area was investigated as part of a study of beryllium-bearing tuffs in western Utah. Keg Mountain lies within the western Utah beryllium belt and contains tuff similar in age and composition to that of Spor Mountain and the Thomas Range. Water-laid tuff at Spor Mountain serves as the host rock to large low-grade beryllium deposits, and tuff in the adjacent Thomas Range shows an extensive trace element halo which was produced by the mineralization at Spor Mountain. Mineralized tuff is not known at Keg Mountain, however, and this study was undertaken to assess the influence of other geologic processes on trace element concentration in tuff and to evaluate the mineral potential of the area.

A petrogenetic model for the water-laid tuff was developed by *R*-mode factor analysis. The analysis shows that most of the variation in mineral and trace element content of the tuff can be accounted for by a five-factor model. The five factors are: concentration of major detrital minerals, concentration of minor rare earth-bearing detrital minerals, two stages of diagenesis (zeolitization and feldspathization), and late magmatic concentration(?) of the trace elements Pb, Ga, and Be.

The two detrital factors are interpreted as indicating that erosion and sedimentation have played important parts in influencing the distribution of some minerals and trace elements in the tuff. Local concentration of major detrital minerals produced a detrital facies rich in quartz, potassium feldspar, plagioclase, and iron oxides. The concentration of the elements Ba, Fe, Cu, Mn, Ti, and V was largely controlled by this detrital factor; Ba is probably present in feldspar and the other elements in iron oxides. A second detrital factor concentrated the minor minerals sphene and zircon and operated with an intensity which increased eastward. This factor produced an association of the elements La, Nb, Y, and Zr and a pronounced easterly increase in their abundances. The intensity with which these two detrital factors have operated indicates that they may pose serious problems for geochemical prospecting for heavy metal and rare earth deposits in tuff.

The two stages of diagenesis did not appreciably alter the trace element content of the tuff. The first stage, zeolitization, resulted in a clinoptilolite-rich tuff somewhat enriched with respect to Sr and impoverished with respect to U. Advanced diagenesis, marked by feldspathization, did not alter the trace element composition of the tuff. Regions of most intense diagenesis are located in the western and southeastern parts of the Keg Mountain area. Clinoptilolite and potassium feldspar are especially abundant in the western part of the range, and clinoptilolite is abundant in the southeastern part of the range. The diagenesis is similar to that which affected tuff in the Thomas Range and is believed to result from alkaline waters derived from leaching of glass.

Three criteria indicate that there is little chance of finding beryllium or fluorspar deposits near Keg Mountain that are similar to those at Spor Mountain: (1) very little fluorite and hydrothermal clay are present; the montmorillonoid clay which occurs in vitric tuff contains no anomalous trace element concentrations and is probably the product of diagenesis; (2) the frequency distribution for Be is not highly skewed, in contrast to the highly skewed distribution for Be in tuff of the Thomas Range, and no anomalous concentrations of Be could be detected by trend surface analysis; and (3) Be was found by *R*-mode factor analysis to be associated with Pb and Ga, in contrast to the Thomas Range tuff in which Be is strongly associated with F, Cs, Li, Ga, Nb, and Y, and not associated with Pb. The association Pb-Be-Ga may be due to the concentration of these elements in the parent rhyolite magma; it is probably not the signature of beryllium-fluorite mineralization.

INTRODUCTION

Keg Mountain lies within the beryllium belt of western Utah that extends from the Sheeprock Mountains into Nevada (Cohenour, 1963) (fig. 1). Water-laid tuff of Pliocene age crops out extensively around Keg Mountain, where its deposition followed a period of ash-flow eruption and caldera collapse (Shawe, 1972). The tuff occupies the same stratigraphic position as similar water-laid tuff of the Thomas Range and Spor Mountain, where it provided the host rock for beryllium and fluorite mineralization (Staatz and Griffitts, 1961; Shawe, 1968). The beryllium-fluorite mineralization at Spor Mountain has produced extensive areas of argillic and feldspathic altered tuff (Lindsey and others, 1973) and has imprinted a large trace element halo on adjacent water-laid tuff in the Thomas Range (Lindsey, 1975). These facts suggested that the water-laid tuff of the Keg Mountain area should be examined for evidence of beryllium-fluorite mineralization.

An investigation of the water-laid tuff of the Keg Mountain area showed no evidence for beryllium-fluorite

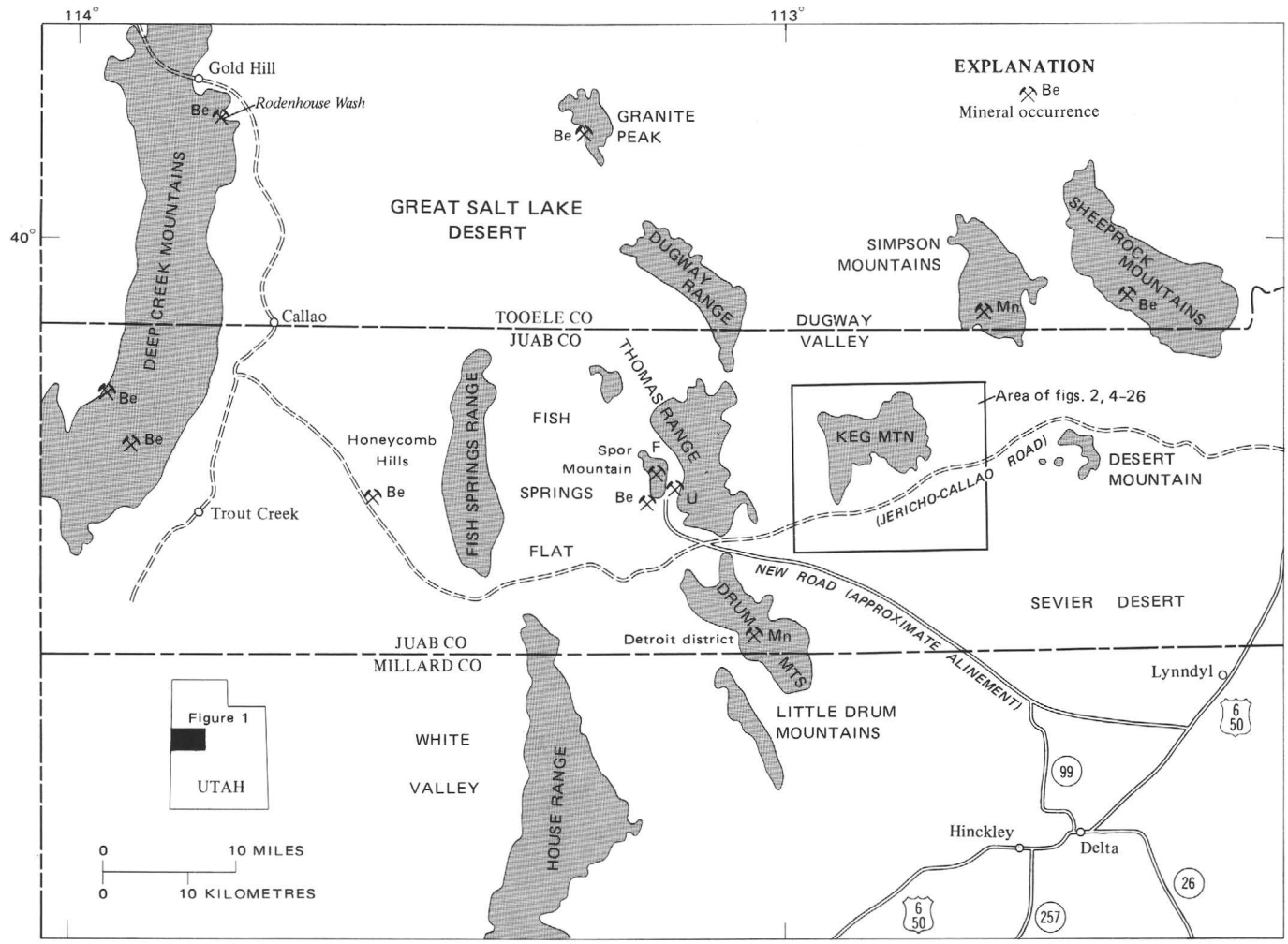

FIGURE 1. — Location of the Keg Mountain study area, other geographic features, and mineral occurrences in the western Utah beryllium belt.

or any other type of mineralization. Analyses for trace elements did reveal generally high concentrations of Be, Ga, Nb, and eU in the water-laid tuff and overlying alkali rhyolite, indicating that these rocks may be classified with other beryllium-bearing volcanics in western Utah. Statistical analysis of the mineralogic and trace element data on the water-laid tuff indicates the influence of numerous other petrogenetic processes, notably those related to the concentration of detrital minerals (erosion and sedimentation) and diagenesis. The purpose of this report is to present a model for the mineral and trace element associations produced by sedimentation and diagenesis in the beryllium-bearing tuffs. This model should serve as a basis for comparison with the model for mineralized tuff (Lindsey, 1975); such comparisons should lead to more accurate identification of regional mineral resource potential from trace element anomalies in tuff. Data used in preparing this report are available from the U.S. Department of Commerce, National Technical Information Service, Springfield, Va. 22161 (Lindsey and others, 1974).

I thank D. R. Shawe for information regarding the geology of the Keg Mountain area, and J. J. Connor, George Van Trump, Jr., and Josephine Boerngen, all of the U.S. Geological Survey, for assistance with statistical analysis and computer programming. Many other employees of the U.S. Geological Survey assisted in the laboratory and made chemical analyses; they are acknowledged in table 2.

GEOGRAPHIC AND GEOLOGIC SETTING

Keg Mountain lies in the Basin and Range province in Juab County, Utah (fig. 1). It is actually a small range that consists of two parts separated by Keg Pass. The mountains west of Keg Pass are low and extend south of the Jericho-Callao road; those east of Keg Pass comprise the highest part of the range.

The stratigraphic section at Keg Mountain (table 1) consists mainly of Tertiary volcanics; these overlie Precambrian and Paleozoic sedimentary rocks along the northern edge of Keg Mountain (Erickson, 1963; Shawe,

TABLE 1. — *Stratigraphic section in the Keg Mountain area*

[Adapted from Shawe (1972); ages are from author's unpublished data; query(?) indicates thickness unknown]

Age	Rock unit	Maximum thickness (ft)	(m)
Pliocene	Younger volcanic group: Alkali rhyolite.	1,000	305
	Water-laid tuff.	100	30
	——— Unconformity ———		
	Rhyolite of Keg Mountains.	1,000	305
	Unconformity		
Oligocene	Middle volcanic group: Rhyolitic welded ash-flow tuff.	500	152
	Quartz-latitic welded ash-flow tuff.	200	61
	Unconformity (?)		
Eocene	Older volcanic group: Latitic and andesitic flows.	?	?
	Unconformity		
Paleozoic and Precambrian	Marine sedimentary rocks.	?	?

1972). The older volcanic rocks consist of (1) latitic and andesitic flows, (2) quartz-latitic welded ash-flow tuff, and (3) rhyolitic welded ash-flow tuff. These rocks were deposited prior to the collapse of the Keg caldera (Shawe, 1972). The rhyolite, water-laid tuff, and alkali rhyolite of Keg Mountain overlie the older volcanic rocks and were deposited after caldera collapse.

The distribution of water-laid tuff is shown in figure 2 and was compiled from the field notes of D. R. Shawe. The tuff overlies an erosional surface of low relief and is typically overlain by alkali rhyolite flows. The base of the alkali rhyolite commonly contains a thin brecciated zone; black vitrophyre is present at the base of the rhyolite east of Keg Pass. The tuff exceeds 100 feet (30 m) in thickness in very few localities and is missing beneath the alkali rhyolite at some localities. It is cut by faults in a few places, notably in the southwestern and southeastern parts of Keg Mountain.

METHODS OF STUDY

SAMPLING PLAN

Water-laid tuff throughout the area of Keg Mountain was sampled for this study. A stratified random sampling plan (Krumbein and Graybill, 1965, p. 156–157), similar to that employed for study of water-laid tuff in the Thomas Range (Lindsey, 1975), was used as a basis to select samples. Each sampling station was chosen randomly from 100 possible locations within each linear mile (1.6 km) of tuff outcrop. In practice, stations were moved laterally to the nearest good exposure of tuff so that samples could be obtained at every sampling station. A few stations were added to fill gaps left by the sampling plan. The stratigraphic thickness of tuff at each station was estimated in the field, and four 1-foot (0.3-m) intervals were selected from random number tables for sampling. The sampling program resulted in 172 samples being collected from 43 stations. The samples consisted of fresh chips and averaged about 2 lbs (0.9 kg).

LABORATORY PROCEDURE

Twenty samples were selected at random for splitting before any other laboratory procedures were begun. These splits and the original 172 samples were placed in random order prior to sample preparation. Samples were split to allow estimation of laboratory errors from replicate measurements on the same sample. The sample population was treated randomly to insure that analytical drift and other laboratory effects did not produce undesirable manmade trends in the data. A specimen for thin sectioning was removed from each sample before splitting and randomization.

All 172 samples plus the 20 additional splits were ground to finer than 60 mesh; approximately 120 g was split from each sample and ground to finer than 100 mesh. Splits of approximately 3 g and 2 g were then removed for X-ray diffraction and spectrographic determinations, respectively; a split of about 10 g was used for eU measurement.

Mineral quantities were estimated by X-ray diffraction. The method is an application of established principles (Klug and Alexander, 1954; Schultz, 1964; Tatlock, 1966) and is the same as that used for study of tuff in the Thomas Range (Lindsey, 1975). Three grams of each sample was ground 15 minutes in a shatterbox and mounted by the backpack mounting technique of McCreery (Klug and Alexander, 1954, p. 300–302). Standards were prepared and X-rayed in the same manner, so that the diffraction intensity of each mineral could be converted into percent. Amorphous glass and poorly crystallized minerals detected by X-ray diffraction were estimated by difference; that is, by adding all other components and subtracting the total from 100.

All trace elements were determined by direct reader spectrometric analysis (Havens and Myers, 1973). Equivalent uranium (eU) was determined by a radiometric counting method based on the assumption that all beta and gamma radiation comes from decay of uranium. Although eU includes effects from such isotopes as ^{232}Th and ^{40}K, previous comparison of eU and chemical uranium in similar tuff indicates that much of the measured eU is due to uranium decay (Staatz and Carr, 1964, p. 115).

COMPOSITION OF THE WATER-LAID TUFF

LITHOLOGY AND PETROGRAPHY

The tuff of Keg Mountain was termed "water-laid" by Shawe (1972) because of its stratified aspect (fig. 3*A*). The tuff contains abundant clasts derived from older volcanic rocks (fig. 3*B*); generally the clasts are only a few inches in diameter, but individuals as much as 16 feet in diameter were observed at one locality in the southeastern part of Keg Mountain. Fragments of older sedimentary rocks were not observed. Massive tuff of

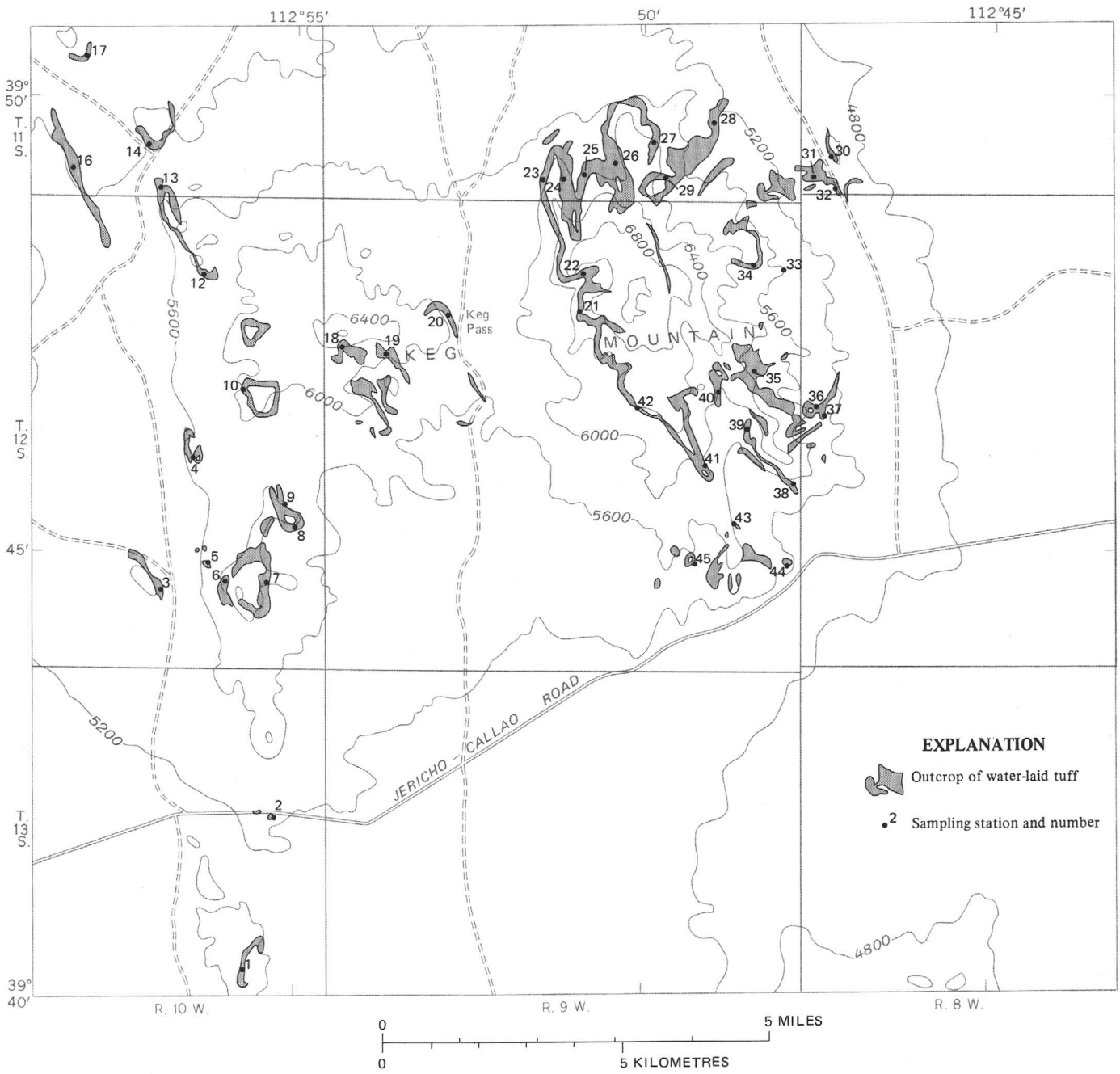

FIGURE 2. — Geographic features, distribution of water-laid tuff, and sampling stations in the Keg Mountain area.

probable air-fall origin is also present; in the eastern half of Keg Mountain the uppermost part of the tuff is commonly welded and overlain by dark vitrophyre (figs. 3*C*, *D*).

The tuff is composed mainly of pumice, volcanic rock fragments, and pyroclastic crystals set in a matrix of glass shards, clinoptilolite, and fine-grained potassium feldspar, quartz, and cristobalite. Crystals of quartz, sanidine, and plagioclase together comprise about 5–15 percent of the tuff; they are euhedral and commonly broken by transport. The tuff contains 1–2 percent each of biotite, magnetite, and hematite, and lesser quantities of sphene, hornblende, augite, zircon, and apatite. Euhedral shapes, often broken, are common for most of these minerals; sphene and augite grains are mainly angular, however. Iron minerals are partially oxidized to a red color, and locally hematite is the only iron oxide present. Calcite, montmorillonoid clay, and trace amounts of fluorite(?) are present in a few samples.

The tuff can be divided into three facies according to

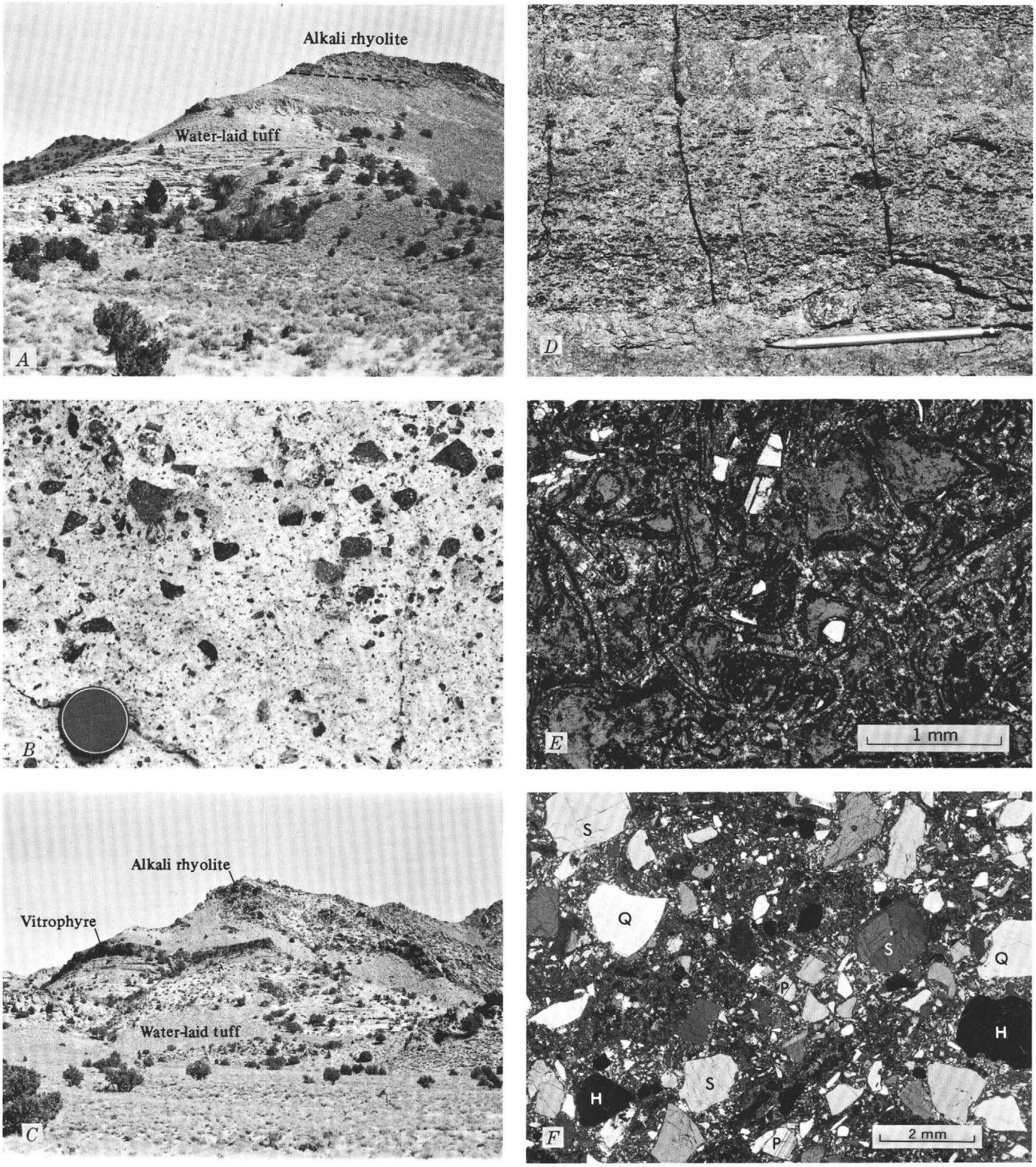

FIGURE 3. — Water-laid tuff in the Keg Mountain area: *A*, section of water-laid tuff overlain by alkali rhyolite, north of station 4; note conspicuous stratification in tuff. *B*, detail of water-laid tuff, showing angular volcanic rock fragments; same outcrop as *A*. *C*, section of water-laid tuff overlain by vitrophyre at station 39. *D*, detail of welded zone in top of water-laid tuff, same outcrop as *C*. *E*, photomicrograph of zeolitic facies at station 43, showing relict shards replaced by clinoptilolite of diagenetic origin (plain light). *F*, photomicrograph of detrital facies at station 42, showing abundant quartz (Q), sanidine (S), plagioclase (P), and hematite (H) derived from underlying volcanic rocks and set in a fine-grained matrix of potassium feldspar and α-cristobalite of diagenetic origin (crossed polars).

gross mineralogy: vitric, zeolitic, and feldspathic (fig. 4). The vitric facies retains a large proportion of unaltered glass pumice and shards and represents the original mineralogy of the water-laid tuff. The zeolitic facies contains clinoptilolite of diagenetic origin (fig. 3*E*) that comprises nearly 100 percent of some samples. The feldspathic facies contains abundant fine-grained potassium feldspar, quartz, and α-cristobalite of diagenetic origin. The tuff at two stations, 17 and 42, also contains abundant quartz and potassium feldspar of detrital origin. The vitric facies is widely distributed through the central and northeastern parts of Keg Mountain; the zeolitic facies occupies much of the western and southeastern parts of the range; the feldspathic facies is present in the center of the western part of Keg Mountain and along certain horizons in the tuff of the northeastern part of the range, where fine-grained quartz, potassium feldspar, dioctahedral montmorillonoid clay, and glass occur together. Cross sections (fig. 4) show a complex pattern of facies arrangement. The

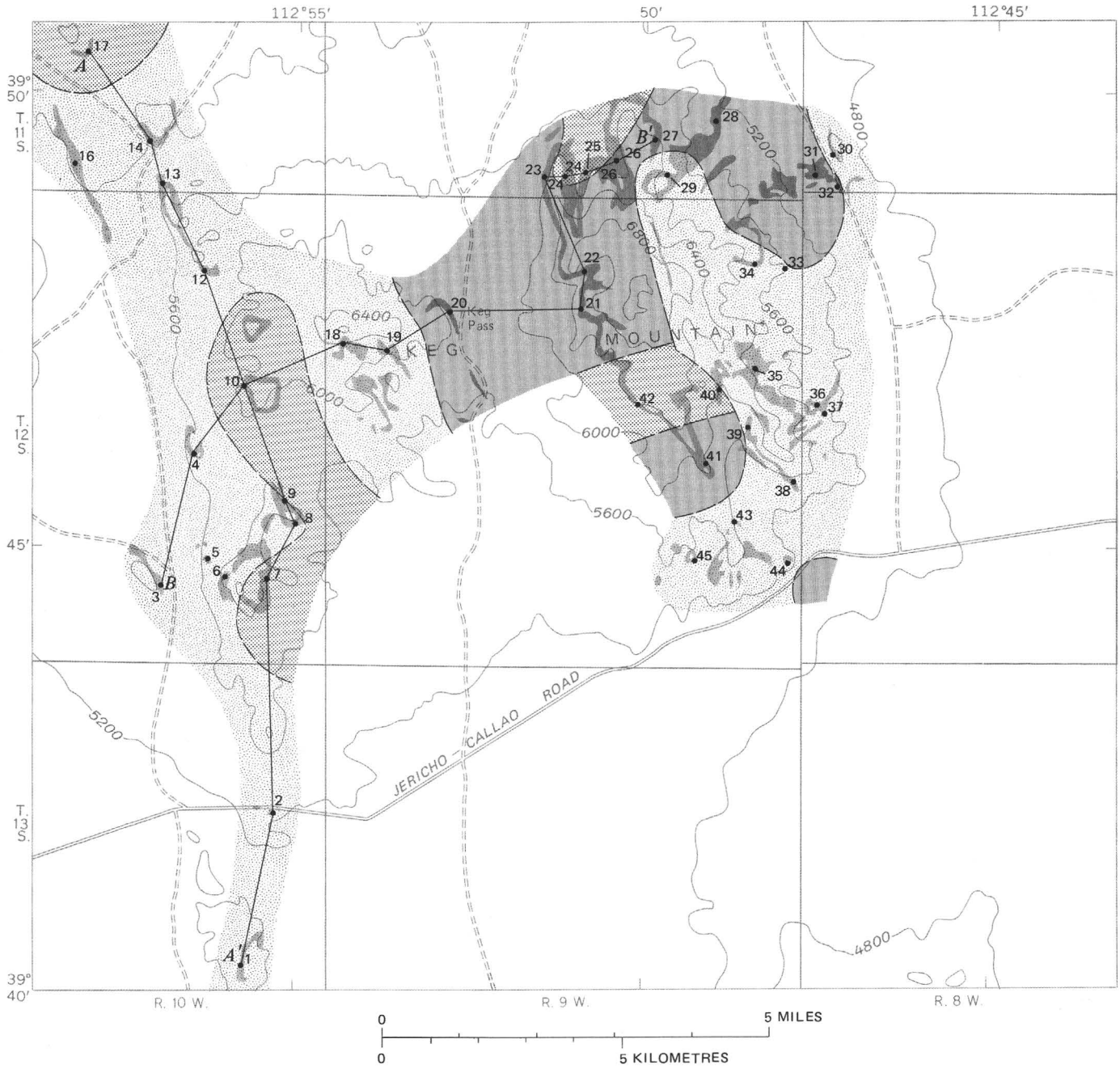

FIGURE 4. — Map and cross sections showing classification

zonation of vitric-zeolitic-feldspathic facies inward from the margins of the range, which is well developed in the Thomas Range (Lindsey, 1975), is evident only in the western part of Keg Mountain. No zoning pattern is evident in the eastern part of the range, although the mineral facies there do tend to follow stratigraphic horizons.

The occurrence of abundant detrital constituents at stations 17 and 42 indicates a fourth facies of detrital origin; this facies overlaps the various diagenetic facies in extent. The tuff at these localities contains as much as 35 percent euhedral and broken crystals of volcanic quartz, sanidine, and plagioclase in a matrix of glass, fine-grained potassium feldspar, and α-cristobalite (fig. 3*F*). Brown biotite and iron oxide minerals are also conspicuously abundant (2–3 percent). Numerous large clasts of gray rhyolite with conspicuous phenocrysts of quartz and plagioclase are present in the tuff at station 42; these clasts were derived from the underlying rhyolite (rhyolite of Keg Mountain of Shawe, 1972). Abundant devitrification products, including α-cristobalite and potassium feldspar, indicate that diagenesis was also important in forming the feldspathic tuff at these two localities. Indications of the detrital facies were also observed at stations 14 and 35, where lesser quantities of crystals, including plagioclase, were observed in thin sections. Large clasts of the rhyolite of Keg Mountain are abundant in the lower part of the tuff at station 35. The scattered occurrence of a few percent plagioclase at many other localities may indicate the influence of erosion and sedimentation.

Little evidence of hydrothermal alteration was found. The beryllium deposits in tuff at Spor Mountain are associated with abundant fluorite and montmorillonoid

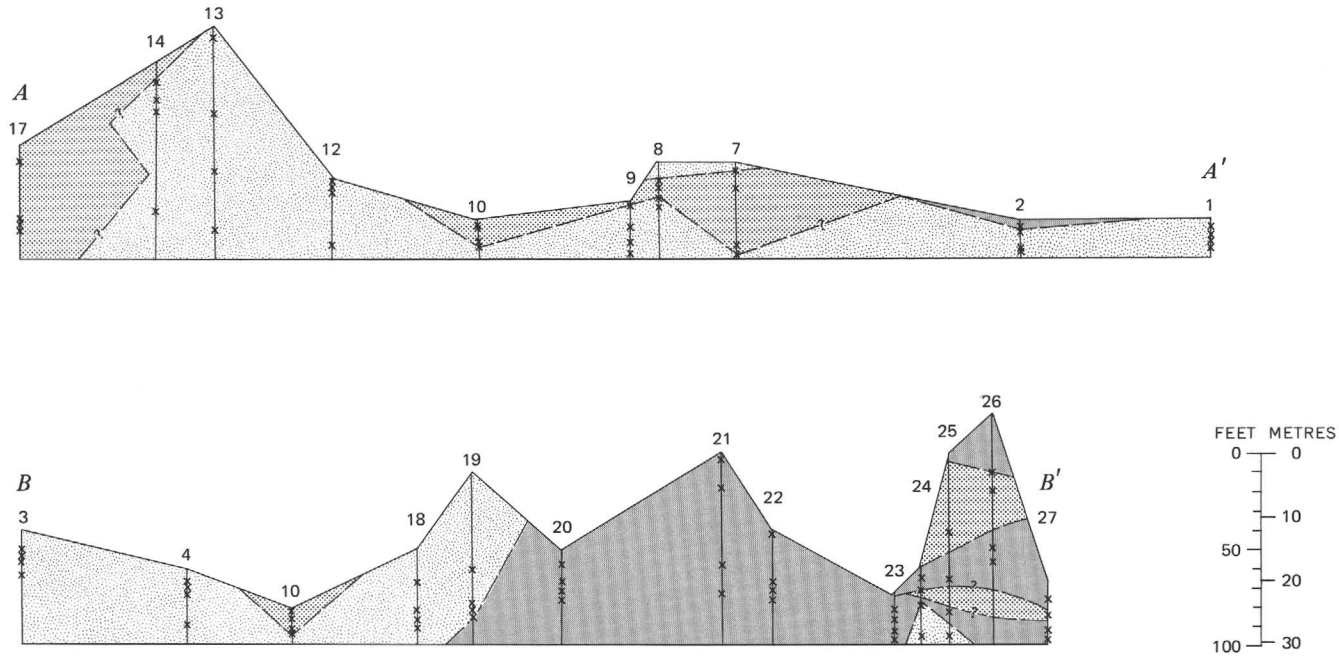

of water-laid tuff into vitric, zeolitic, and feldspathic facies.

clay. Very little fluorite was detected in the tuff of the Keg mountain area, however, and the montmorillonoid clay which is widely distributed is probably of diagenetic origin. The lowermost outcrop of tuff at station 19 is much altered to dioctahedral montmorillonoid clay, but spectrographic analyses failed to reveal evidence of mineralization. Samples from prospect pits in tuff near stations 13 and 30 were examined for evidence of alteration or mineralization; no clay minerals, fluorite, or anomalous trace element concentrations were found.

ABUNDANCE OF MINERALS AND TRACE ELEMENTS

The mineral and trace element compositions of the tuff are summarized in table 2. Although no analyses for major chemical constituents were made, the composition of the tuff is probably rhyolitic, similar to that of the water-laid tuff in the Thomas Range (Lindsey, 1975). The trace elements Be (5 ppm), Ga (26 ppm), Nb (29 ppm), and U (33 ppm eU) are probably more abundant than in other tuffaceous and volcanic rocks, although Be, Ga, and U are less abundant than in the water-laid tuff of the Thomas Range.

The frequency distributions of each mineral and trace element (hereafter referred to collectively as variables) are summarized by moment estimates and histograms (Freund, 1960, p. 3–105). Central tendency was estimated by the arithmetic and geometric means and by the median (50th percentile); variation was estimated by the standard deviation, geometric deviation, and the difference between the 10th and 90th percentiles (table 2). Estimates of means and variation for censored frequency distributions — that is, where the concentration of a particular mineral or element is below the limit of detection for some samples — were made by the methods of Cohen

TABLE 2. — *Summary statistics for mineral and trace element composition of 172 samples of water-laid tuff from the Keg Mountain area*

[Mineral composition determined by X-ray diffraction by K. A. Buzard; equivalent uranium (eU) determined by beta-gamma scaler by E. J. Fennelly; Li determined by six-step semiquantitative spectrographic analysis by L. D. Forshey; all other elements determined by direct reading spectrograph by R. G. Havens, N. M. Conklin, and L. M. Lee. Elements looked for but not found, with their detection limits in parts per million, are Ag (4), Au (20), Bi (20), Cd (100), Co (8), Ge (100), In (20), Mo (20), Pd (10), Re (70), Sb (300), Tl (50), W (500), and Zn (300). Leaders indicate not calculated]

Mineral or trace element	Number of samples below the limit of detection	Lower limit of detection	Geometric mean[1]	Geometric deviation[1]	Percentile		
					10th	50th	90th
			Mineral composition (weight percent)				
Montmorillonoid clay	139	10	---	---	---	---	13.0
Mica	99	1	---	---	---	---	2.2
Clinoptilolite	61	5	[2]19.9	4.81	---	49.0	83.2
Quartz	0	1	12.1	1.62	6.0	12.6	24.2
α-cristobalite	17	1	3.7	2.56	2.2	3.8	12.1
K-feldspar	0	1	19.9	1.65	9.7	20.1	38.3
Plagioclase	164	5	---	---	---	---	---
Calcite	157	1	---	---	---	---	1.0
Fluorite	162	0.5	---	---	---	---	---
Glass	121	30	---	---	---	---	62
			Trace element composition (parts per million)				
B	169	30	---	---	---	---	---
Ba	1	10	160	2.39	51	170	577
Be	11	4	5.2	1.27	4.1	5.6	7.8
Cr	147	5	---	---	---	---	5.0
Cu	0	1	3.7	1.62	2.1	4.2	6.2
Fe	0	500	7,219	1.46	4,264	7,038	11,650
Ga	0	10	26.1	1.14	21.5	25.6	31.0
La	38	50	57.4	1.47	---	57.8	86.0
Li	151	50	---	---	---	---	50
Mn	0	7	332	1.56	185	342	554
Nb	8	20	*28.6*	*4.8*	21.7	29.5	36.3
Ni	171	7	---	---	---	---	---
Pb	6	20	29.3	1.27	19.4	29.1	37.3
Sc	170	10	---	---	---	---	---
Sn	171	20	---	---	---	---	---
Sr	0	10	302	2.33	86	319	926
Ti	0	20	1,001	1.53	585	961	1,753
eU	1	10	*33.4*	*9.2*	25.3	38.6	49.5
V	73	10	10.9	1.67	---	10.0	22.8
Y	47	20	26.0	1.43	---	25.2	38.1
Zr	0	20	112	1.25	87	107	158

[1]Italics indicate arithmetic mean and standard deviation.
[2]Bimodal distribution.

and Sichel (Miesch, 1967a, p. B5–B8). Statistical parameters were not computed for variables for which more than 30 percent of the samples are below the limit of detection, although data for some are summarized later in histograms and maps.

Study of the skewness revealed that frequency distributions for most variables depart significantly from the normal model. Normal distributions are symmetrical with a skewness near 0 and if the frequency distribution deviates significantly from the normal, various transformations of the data (Miesch, 1967a, p. B5) are necessary before further statistical analysis. Logarithmic transformations were helpful in normalizing the data for all variables except Nb and eU; the frequency distributions of these two variables were found to be nearly normal without transformation. Transformation of data to logarithms prior to other statistical calculations is indicated in the tables following table 2 by referring to variables as "log clinoptilolite," etc. The geometric mean and geometric deviation are given in table 2 as estimates of central tendency and variation for those variables which tend to exhibit log normal frequency distributions. They are the antilogarithms of the arithmetic mean and standard deviation of the log concentrations. The arithmetic mean and standard deviation of Nb and eU are given in table 2 as the best estimate of central tendency and variation for these two variables.

Histograms, or bar diagrams, were constructed for most variables (figs. 5–26). The data were divided into classes of equal width for normally distributed data and into geometric classes for log normal data. The geometric class interval was usually selected so that six classes per order of magnitude were plotted, with the series 1, 1.5, 2, 3, 5, 7, 10, etc. serving as class midpoints. For Ga and Zr, as many as 20 classes per order of magnitude were necessary to display the data adequately (figs. 16, 26). The histogram for Be (fig. 12) is based on arithmetic classes because that trace element was reported as integers in the range of 4–9 ppm.

SOURCES OF VARIATION

The total variance of each mineral and trace element can be understood as the sum of numerous sources of natural and manmade variation. The observed value of each measurement is influenced by each of these sources of variation. The magnitude of each of these sources of variation can be determined by analysis of variance. In this study, the sampling design outlined earlier provides the basis for a three-level nested analysis of variance (Krumbein and Graybill, 1965, p. 215).

The statistical model of variation is:

$$x_{ijk}=\mu+\alpha_i+\beta_{ij}+\gamma_{ijk},$$

where x_{ijk}=the kth measurement on the jth sample from the ith station where $1\leq k\leq 2$, $1\leq j\leq 4$, and $1\leq i\leq 43$. Thus each measurement may be viewed as the sum of a grand mean (μ) and deviations introduced by a particular station (α_i), sample (β_{ij}), and laboratory measurement (γ_{ijk}). The latter term is identified with laboratory error and the preceding term (β_{ij}) may be called sampling error. A more extensive discussion of sampling models in geochemistry is given by Miesch (1967b).

Analysis of variance was used to partition the total variance of each variable into three components; these components are assigned to variance among stations (s_α^2), among samples within stations (s_β^2), and among splits within samples (s_γ^2) (table 3). The analysis is based on the assumptions that α_i, β_{ij}, and γ_{ijk} are random variables with means of zero and variances of s_α^2, s_β^2, and s_γ^2 and that the variance components are additive:

$$s_T^2=s_\alpha^2+s_\beta^2+s_\gamma^2,$$

where s_T^2 is the total variance. Station variance (s_α^2) is a measure of geographic variation; sample variance (s_β^2) is a measure of sampling error; and the split variance, (s_γ^2), is a measure of laboratory error and includes effects due to grinding, splitting, and analytical error.

Calculations for the analysis of variance were made in two stages. In the first stage, a two-level model consisting of 40 splits (20 samples) was used to compute estimates of the among-splits variance component (s_γ^2). In the second stage, another two-level model consisting of all 43 stations and 172 samples was used to compute estimates of the among-stations variance component (s_α^2) and the sum of among-samples and among-

TABLE 3. — *Estimates of total variance, variance components in a three-level nested sampling design, and variance ratios for mineral and trace element composition of water-laid tuff*

[Significant differences (0.05 level) among stations were found for all variables. $V_m=\frac{s_\alpha^2}{(s_\beta^2+s_\gamma^2)/4}$, the ratio of among-stations variance to the variance of the station mean]

Mineral or trace element	Total variance	Components of variance as percent of total variance: among stations (s_α^2)	among samples (s_β^2)	among splits (s_γ^2)	Variance ratios V_m
	(percent)[2]				
Log clinoptilolite	0.466	79	21	<1	15.05
Log quartz	.044	60	25	15	6.00
Log α-cristobalite	.167	38	58	4	2.45
Log K-feldspar	.047	55	31	14	4.89
Log glass	.041	69	27	4	8.90
	(ppm)[2]				
Log Ba	0.144	59	36	5	5.76
Log Be	.011	29	28	43	1.63
Log Cu	.044	22	20	58	1.13
Log Fe	.027	53	38	9	4.51
Log Ga	.003	33	33	34	1.97
Log La	.028	34	24	42	2.06
Log Mn	.037	57	26	17	5.30
Nb	23.5	35	24	41	2.15
Log Pb	.011	23	59	18	1.19
Log Sr	.135	64	33	3	7.11
Log Ti	.034	44	42	14	3.14
eU	85.5	35	<1	65	2.15
Log V	.049	57	36	7	5.30
Log Y	.024	51	3	46	4.16
Log Zr	.010	47	<1	53	3.55

splits variance components ($s_\beta^2+s_\gamma^2$). The among-samples variance component (s_β^2) was determined by difference. Data on total crystalline material were used to estimate the variance components of glass in the analysis; glass has a highly censored frequency distribution and was computed as 100 minus total crystalline material when a glass hump was noted in the X-ray pattern.

The estimates of variance components in table 3 show that two trace elements, Cu and Pb, have only slightly more than a 20 percent geographic (among-stations) variation; the remainder of the variation observed for these elements is due to sampling and laboratory error. The mineral cristobalite and the trace elements Be, Ga, La, Nb, and U (as eU) also exhibit weak geographic variation. All other minerals and the trace elements Ba, Fe, Mn, Sr, V, and Y have a large (>50 percent) geographic-variance component.

Variation among samples (sampling error) in the design is equivalent to small-scale stratigraphic variation, since each station consists of four samples drawn at random from a stratigraphic section through the tuff. Thus the large (>50 percent) among-samples component of variance observed for cristobalite and Pb may be interpreted as being due to major variation up and down tuff sections. The variance component among splits (laboratory error) is especially large for Cu, eU, and Zr; for Be, La, Nb, and Y it also approaches 50 percent of the total variance.

GEOGRAPHIC VARIATION

Regional patterns, or trends, are of special interest in this study because they may be used to help identify petrogenetic processes and to search for evidence of beryllium-fluorite and other mineralization (Lindsey, 1975). The geographic distributions of each variable are shown in figures 5–26. Only presence or absence is noted for calcite, montmorillonoid clay, and fluorite (fig. 10) and Cr and Li (fig. 13). The distributions of all other variables are summarized by symbols for the arithmetic or geometric mean at each sampling station.

The potential for definition of geographic variation was estimated by computing V_m, the ratio of the among-stations variance to the variance of the station mean (table 3) (Connor and others, 1972). In general, V_m values below about 1.00 indicate that the error in any station mean based on four samples is so high that comparisons among stations may be unreliable, and further sampling at each station is necessary if stable maps are to be constructed. Values of V_m above 1.00 indicate greater potential for constructing stable maps. Although the sampling design was adequate to yield a V_m ratio greater than 1.00 for all of the variables measured the ratios for Cu and Pb are near 1.00. Therefore there is some doubt whether any geographic variation of these two trace elements can be detected with the available data. Beryllium and Ga have somewhat higher V_m ratios, but geographic variation of these elements may also be difficult to demonstrate. Clinoptilolite, quartz, potassium feldspar, glass, Ba, Fe, Mn, Sr, V, and Y all show high ratios (≥4.00), indicating a high potential for defining geographic variation.

Polynomial trend surfaces provide an objective method for studying the nature of geographic variation. Methods of least-squares surface fitting are described by Krumbein and Graybill (1965, p. 319–340). Trend surfaces of degrees 1 through 5 were fitted to data for all variables. The model for the 5th degree polynomial is:

$$\hat{x}_{ij}=\beta_{00}+\beta_{10}U_i+\beta_{01}V_j+\beta_{20}U_i^2 +\beta_{11}U_iV_j+\beta_{02}V_j^2+\ldots+\beta_{05}V_j^5,$$

where $\hat{x}_{ij}$ is the predicted value of some variable observed in the sample collected at map coordinates (U_i, V_j). $\hat{x}_{ij}$ has the structure $x_{ij}=\hat{x}_{ij}+e_{ij}$, where x_{ij} is the observed value and e_{ij} is the residual. β_{00}, β_{10}, . . . , β_{05} are the numerical coefficients chosen to minimize the variance of e_{ij}. For polynomials of lesser degree, the number of coefficients and terms is accordingly fewer. Thus it is impossible to partition the variance into two parts: (1) that due to a regional trend as expressed by a polynomial equation and (2) that due to local variation (the residual). The proportion of variance explained by the

TABLE 4. — *Sum of squares of the deviations from the mean and percent reduction of the sum of squares by polynomial surfaces of degree 1 through 5 fitted to data on mineral and trace element composition of 164 samples of water-laid tuff*

[Italic numbers indicate percent reduction of sum of squares above Howarth's (1967) limits for random data (linear, quadratic, and cubic surfaces only). Asterisks (*) indicate significant reduction of the sum of squares (0.05 level)]

Mineral or trace element	Sum of squares	Cumulative percent reduction of sum of squares				
		Linear	Quadratic	Cubic	Quartic	Quintic
	(percent)[2]					
Log clinoptilolite	76.29	*25**	*38**	*42**	47*	50
Log quartz	7.152	2	6	*20**	24	25
Log α-cristobalite	27.42	4*	6	12*	25*	26
Log K-feldspar	7.885	1	6*	*17**	20	26
Log glass	6.783	*21**	*30**	31	34	36
	(ppm)[2]					
Log Ba	24.49	8*	*13**	*33**	38*	39
Log Be	2.032	0	3	11*	14	16
Log Cu	7.063	0	6*	13*	17	21
Log Fe	4.336	0	6*	*19**	22	22
Log Ga	5.514	1	9*	12	19*	20
Log La	5.678	*19**	*20*	*23*	26	27
Log Mn	6.147	2	7*	16*	20	21
Nb	4,084	*13**	*19**	*30**	35*	35
Log Pb	2.040	3	8*	11	14	16
Log Sr	22.08	2	*13**	*20**	27*	*41**
Log Ti	5.340	3	4	12*	15	19
eU	14,093	5*	9	11	14	24*
Log V	6.735	2	*12**	*24**	31*	34
Log Y	4.764	*40**	*41*	*53**	54	54
Log Zr	1.518	*18**	*19*	*23*	27	29

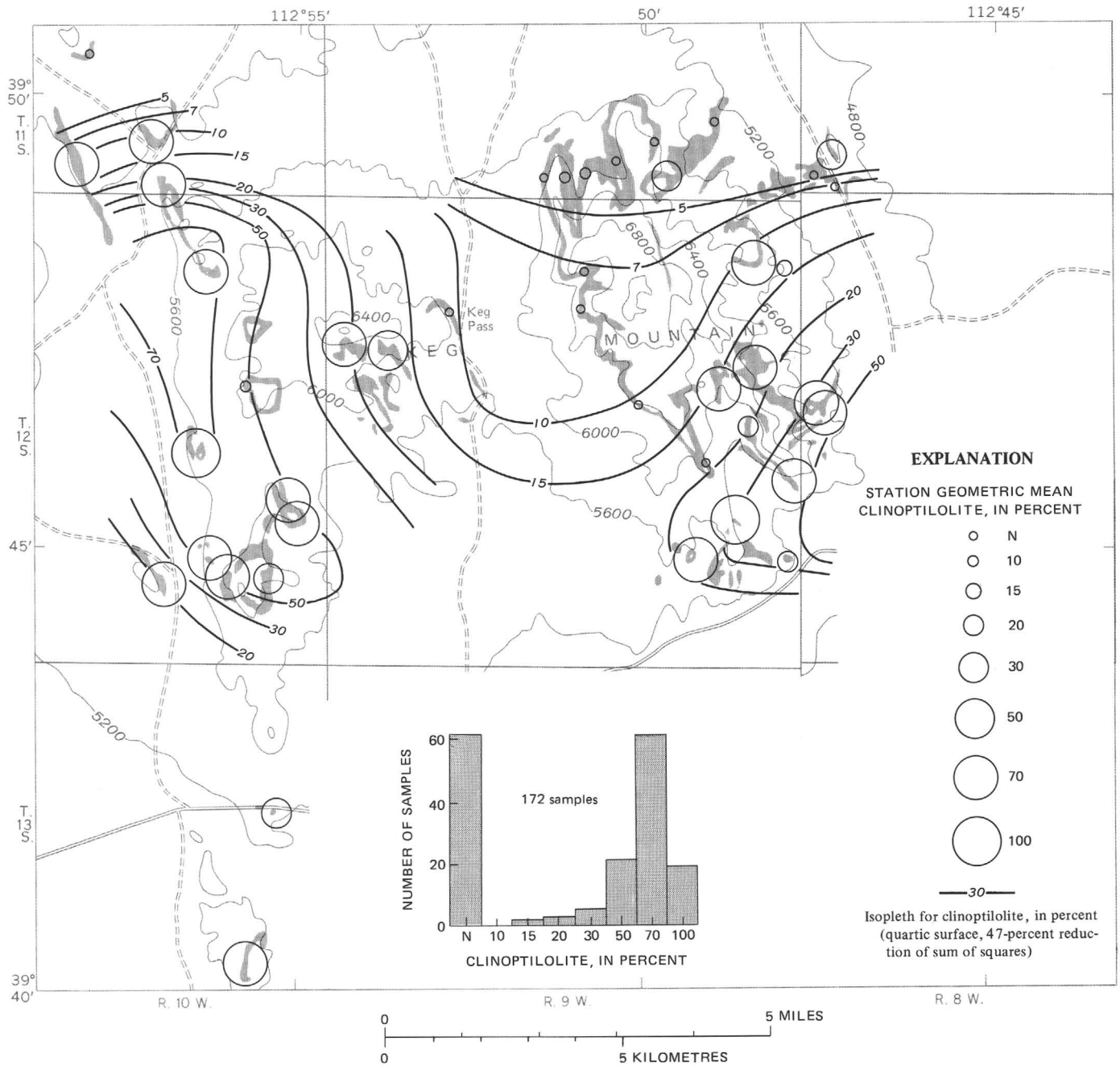

FIGURE 5. — Clinoptilolite content of water-laid tuff in the Keg Mountain area.

trend should not exceed that due to the among-stations variance component listed in table 2.

The relative strengths of the trends fitted to data on minerals and trace elements are presented in table 4. Stations 1 and 2 were omitted from data fitted to trend surfaces because they lie well outside the region covered by the remaining stations. Random effects can also give rise to weak trends, and Howarth (1967) considered that reductions in the percent sum of squares smaller than 6.0, 12.0, and 16.2 for linear, quadratic, and cubic surfaces respectively can be taken as an upper limit for trends which may arise with random data. In the present study, α-cristobalite, Be, Cu, Ga, Mn, Pb, Ti, and eU show weak trends which could be ascribed to random effects. Either linear, quadratic, or cubic trends for the remaining variables account for a sufficiently large percentage reduction of the sum of squares so as to suggest that the trends are real.

Another method of evaluating trend surfaces is by analysis of variance of the sums of squares (Krumbein and Graybill, 1965, p. 333–337). This method was applied, and the percent reduction values marked by

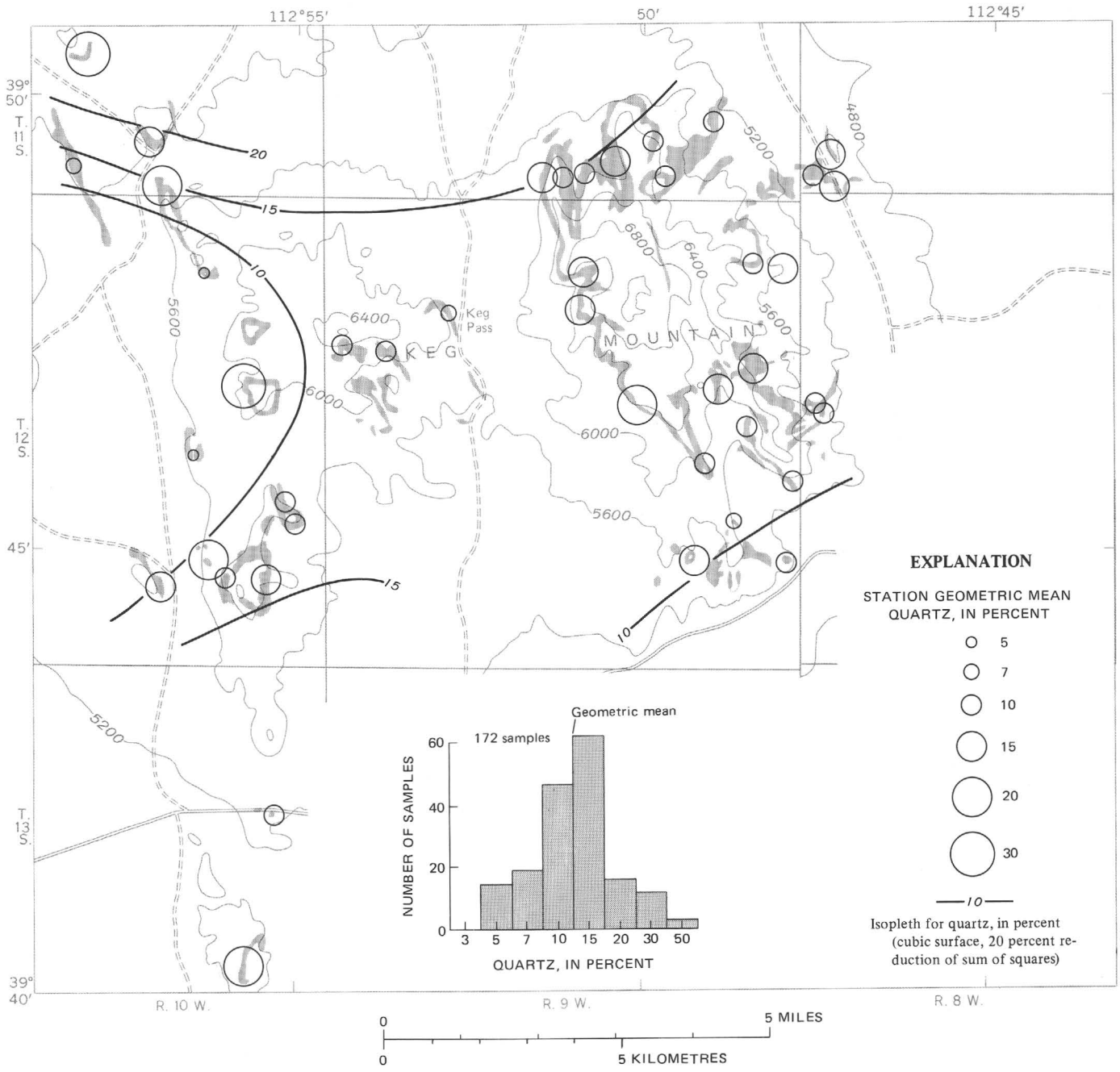

FIGURE 6. — Quartz content of water-laid tuff in the Keg Mountain area.

asterisks (*) in table 4 indicate those surfaces which result in a significant (0.05 level) reduction of the sum of squares. Both Howarth's (1967) limits and analysis of variance were used to select trend surfaces for mapping on figures 5–26. Only variables having surfaces which exceed Howarth's limits were considered for mapping; the highest degree surface which shows a significant reduction in the sum of squares was chosen as the best representation of the geographic trend.

The geographic trends of certain minerals confirm the facies classification presented in figure 4. The constituents clinoptilolite (fig. 5) and glass (fig. 9) show strong trends that parallel the geographic distribution of zeolitic and vitric facies, respectively. Quartz (fig. 6) and potassium feldspar (fig. 8), on the other hand, show relatively weak trends whereas α-cristobalite (fig. 7) shows no significant trend at all; these major detrital and late-stage diagenetic minerals are not distributed as well-defined regional facies, but instead occur largely as local and discontinuous facies.

The absence of any regional trend for beryllium (fig. 12) is noteworthy. The very low reduction of the sum of

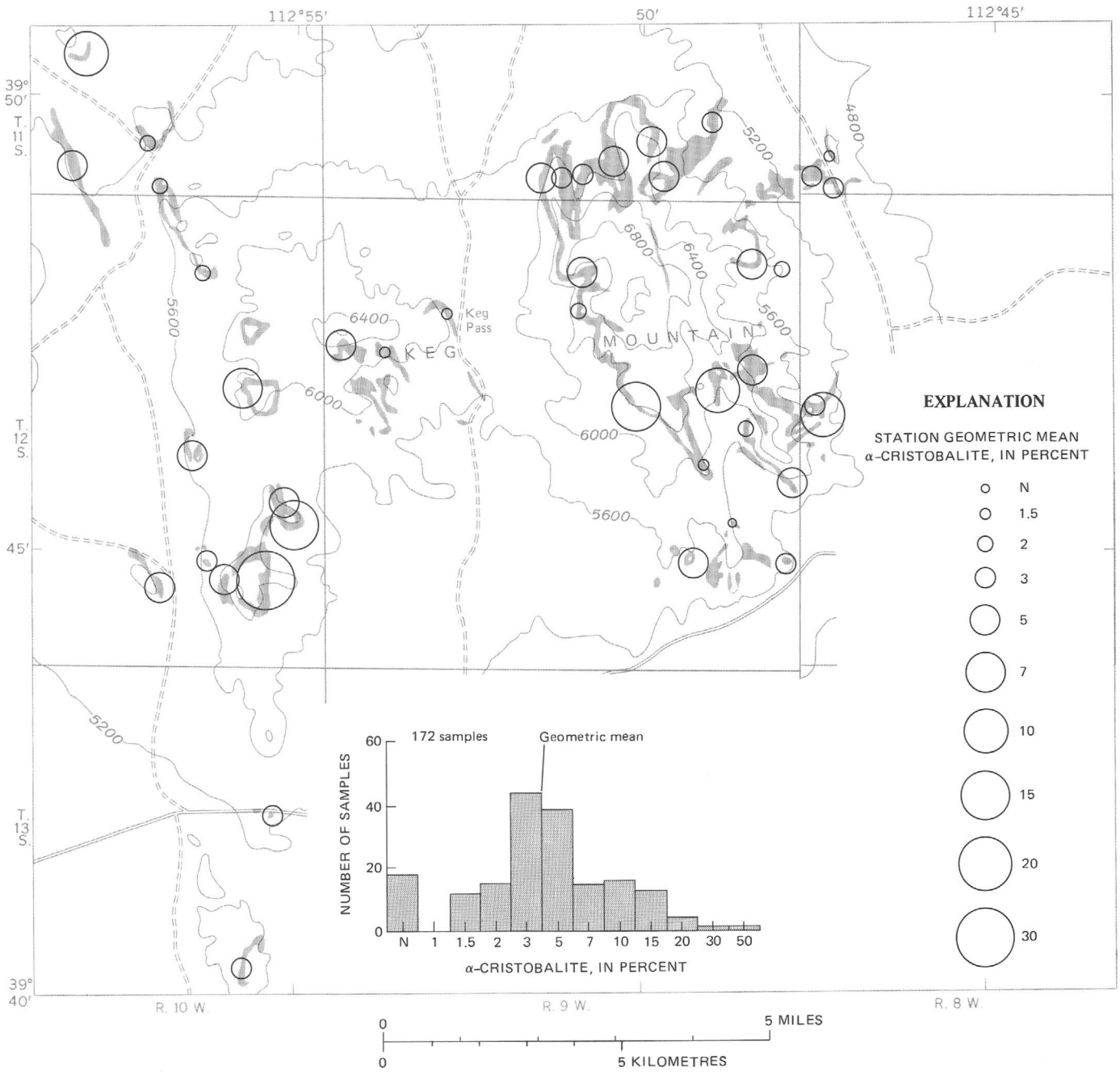

FIGURE 7. — α-cristobalite content of water-laid tuff in the Keg Mountain area.

squares for various trend surfaces fitted to data on beryllium in tuff of the Keg Mountain area indicates that no concentration attributable to mineralization is present. In the southern part of the Thomas Range, polynomial trend surfaces were used to define a pronounced beryllium halo around the Spor Mountain beryllium and fluorspar district (Lindsey, 1975).

The trends for La, Nb, Y, and Zr (table 4; figs. 17, 19, 25, and 26, respectively) are of interest because they exhibit some degree of similarity. All four trace elements have significant linear trends with an easterly increase in concentration. This information anticipates a finding of the next section, that these elements reflect an eastward increase in sphene and zircon.

PETROGENESIS

PROBLEMS IN PETROGENETIC INTERPRETATION

Interpretation of mineralogical and chemical change from bulk rock analyses is complicated by several important considerations. All concentrations are reported as ratios, as either percent or parts per million, and

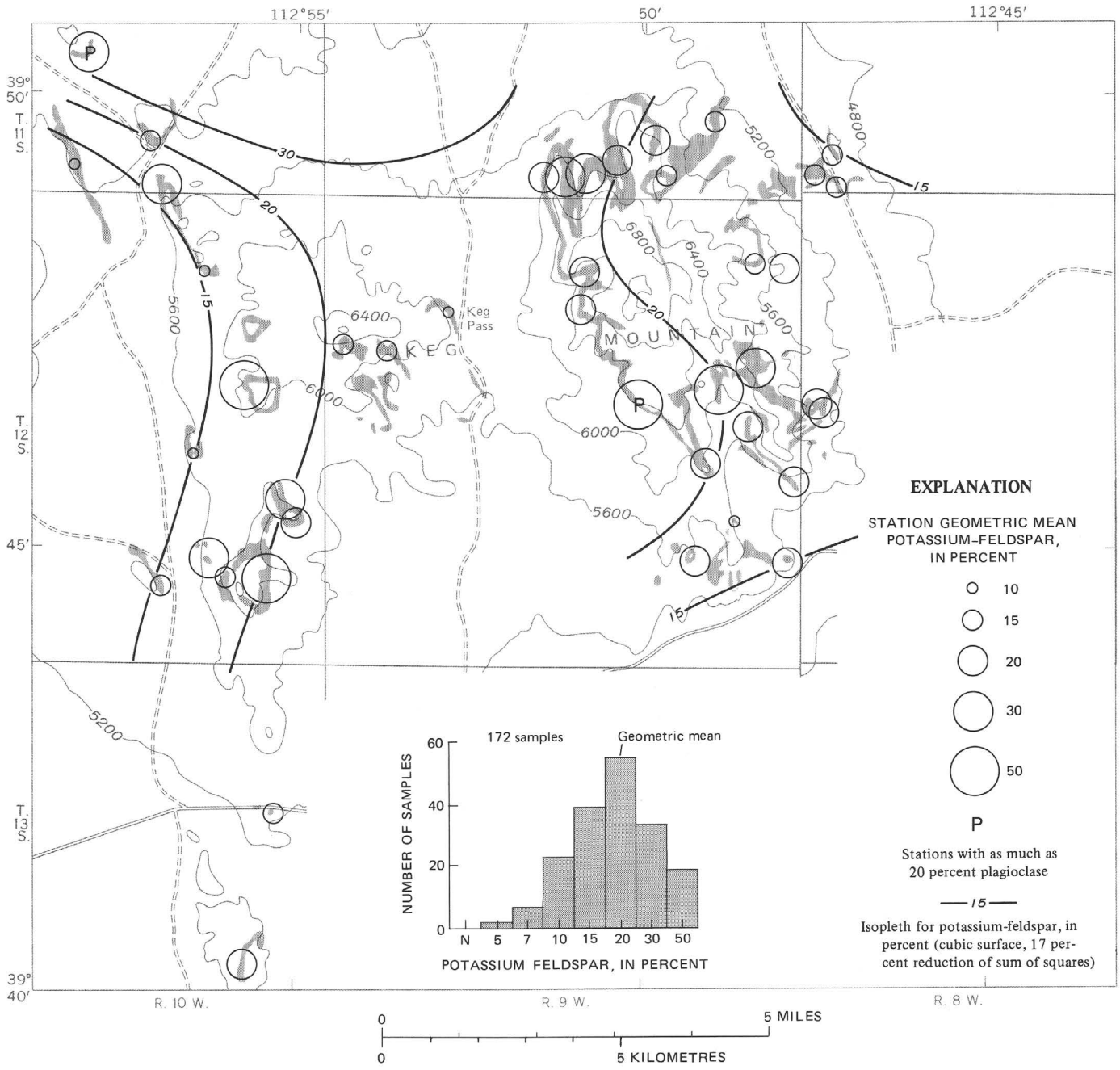

FIGURE 8. — Potassium feldspar content of water-laid tuff in the Keg Mountain area. Also shown is the occurrence of plagioclase.

therefore variations in concentration of minerals and trace elements among samples of a rock type represent changes in the ratios as determined by (1) addition and removal, or (2) residual concentration and dilution of the various constituents. For example, a trace element may be present at unusually high concentrations in some samples of tuff because either it was actually added to the rock or other constituents were removed (residual enrichment). The problem is further complicated by changes in the bulk density and volume of the rock. For example, an increase in bulk density could be due either to exchange of light elements for heavier elements or to addition of constituents by filling of pore space. If compaction of the rock occurred during alteration, the bulk density could decrease without chemical change. These problems are discussed more fully in an earlier paper (Lindsey, 1975).

Percentage and parts per million data also affect the interpretation of correlation among the minerals and trace elements. High positive correlation is usually interpreted as an indication of a common origin, whereas noncorrelation is an indication of independent origin. An

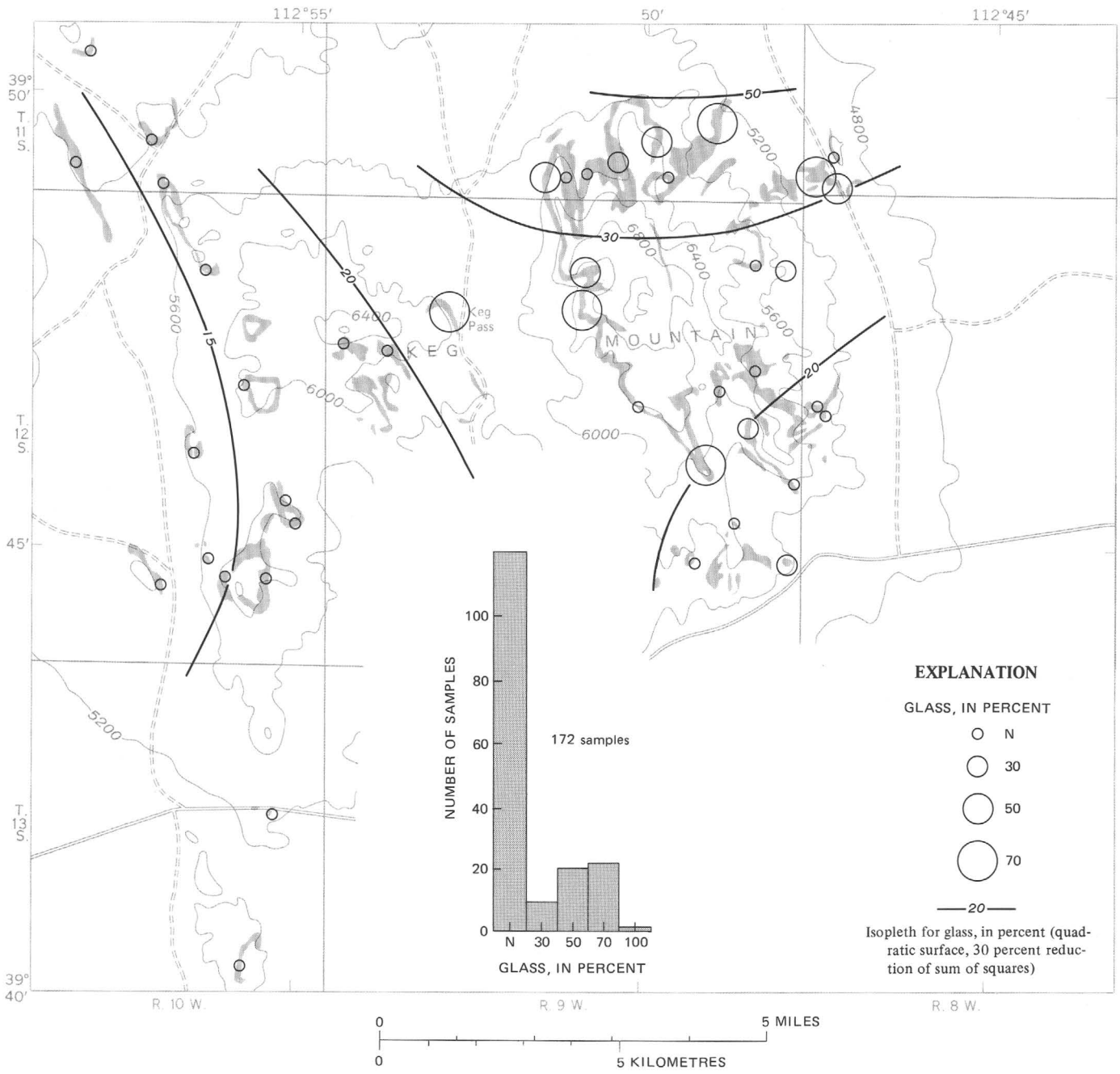

FIGURE 9. — Glass content of water-laid tuff in the Keg Mountain area.

important constraint upon such interpretations is the effect of closure (Chayes, 1960). Data on mineral and chemical constituents form two groups of variables, each of which sum to 100 percent under ideal conditions. In a two-component closed array, one component must increase as the other component decreases, inducing a perfect negative correlation. Similar but more complicated effects exist in multicomponent arrays such as the mineral and trace element composition of the tuff samples. Although there is currently no satisfactory solution to the problem of closure (Miesch, 1969), an attempt will be made in this study to identify its obvious effects on the covariation of major constituents.

A PETROGENETIC MODEL

A petrogenetic model has been proposed for the origin of water-laid tuff in the Thomas Range (Lindsey, 1975). Likewise, the origin of water-laid tuff at Keg Mountain can be stated in terms of a model which accounts for the various petrogenetic processes, or factors, that are believed to have been important in producing the observed mineral and trace element variation. A general

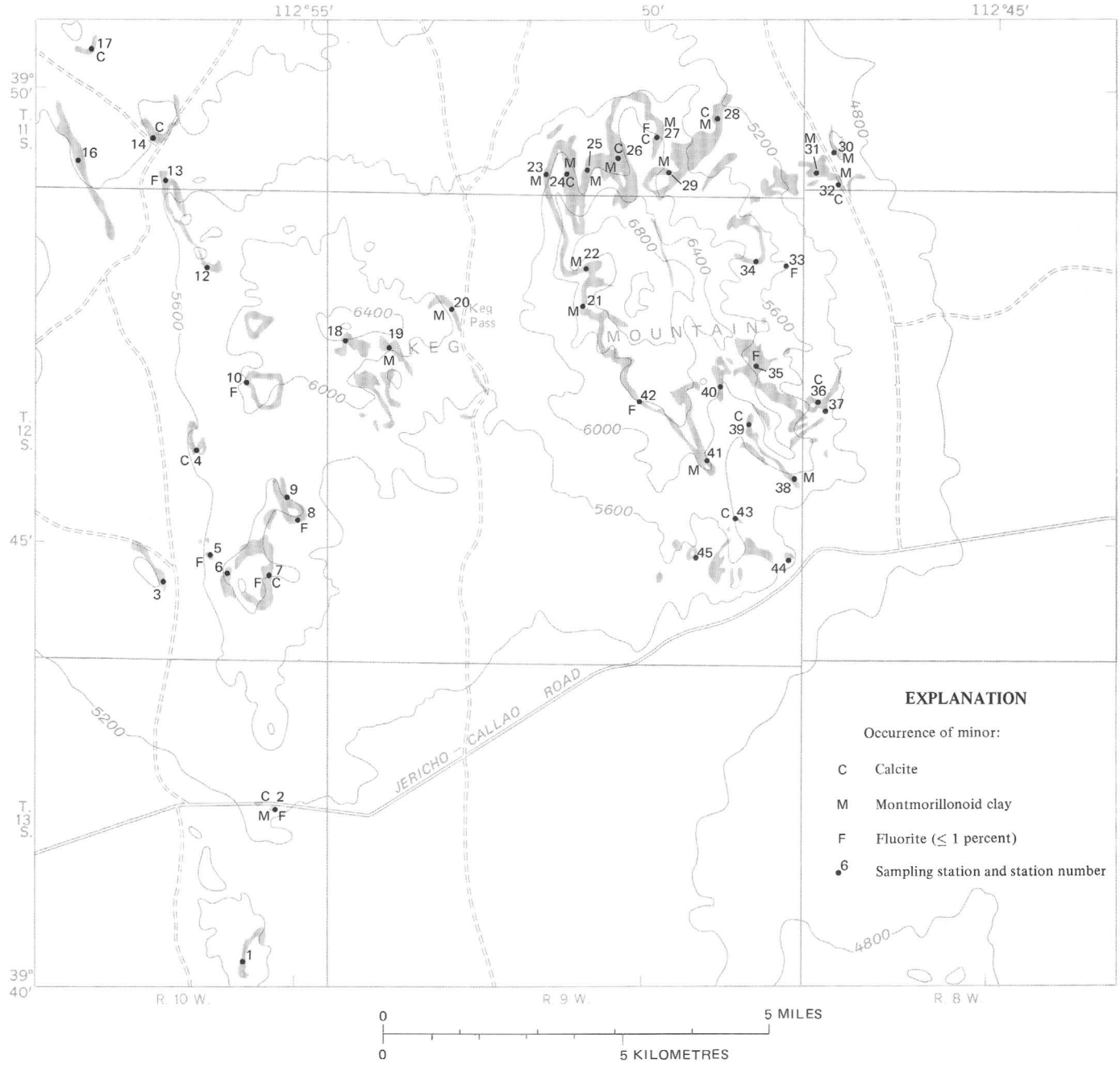

FIGURE 10. — Occurrence of calcite, montmorillonoid clay, and fluorite in the Keg Mountain area.

model may be stated as follows:

$$x_{ji}=\alpha_{j1}F_{1i}+\alpha_{j2}F_{2i}+\ \ldots\ +\alpha_{jp}\ F_{pi}+\alpha_j U_{ji}$$

where x_{ji} is the value of the ith sample for the jth variable and is a linear function of p common factors (F). Each factor (F) operates with an intensity of the coefficients α_{ji}, α_{j2}, . . . , α_{jp}, and U_{ji} is a unique factor accounting for the remaining variation in the data (Cooley and Lohnes,1962, p. 160).

The identity of some of the factors in the general model can be anticipated from information already presented on the petrography and the mineral and trace element content of the water-laid tuff. Processes of erosion and sedimentation obviously were active in forming the detrital facies of crystal-rich tuff; and the processes of zeolitization and potassium feldspar diagenesis are known to have been responsible for corresponding zeolite and potassium feldspar facies in the tuff (fig. 4). The mineralization-related trace elements Be, Ga, and Y are present in lower concentrations in the water-laid tuff of Keg Mountain (table 2) than in the Thomas Range

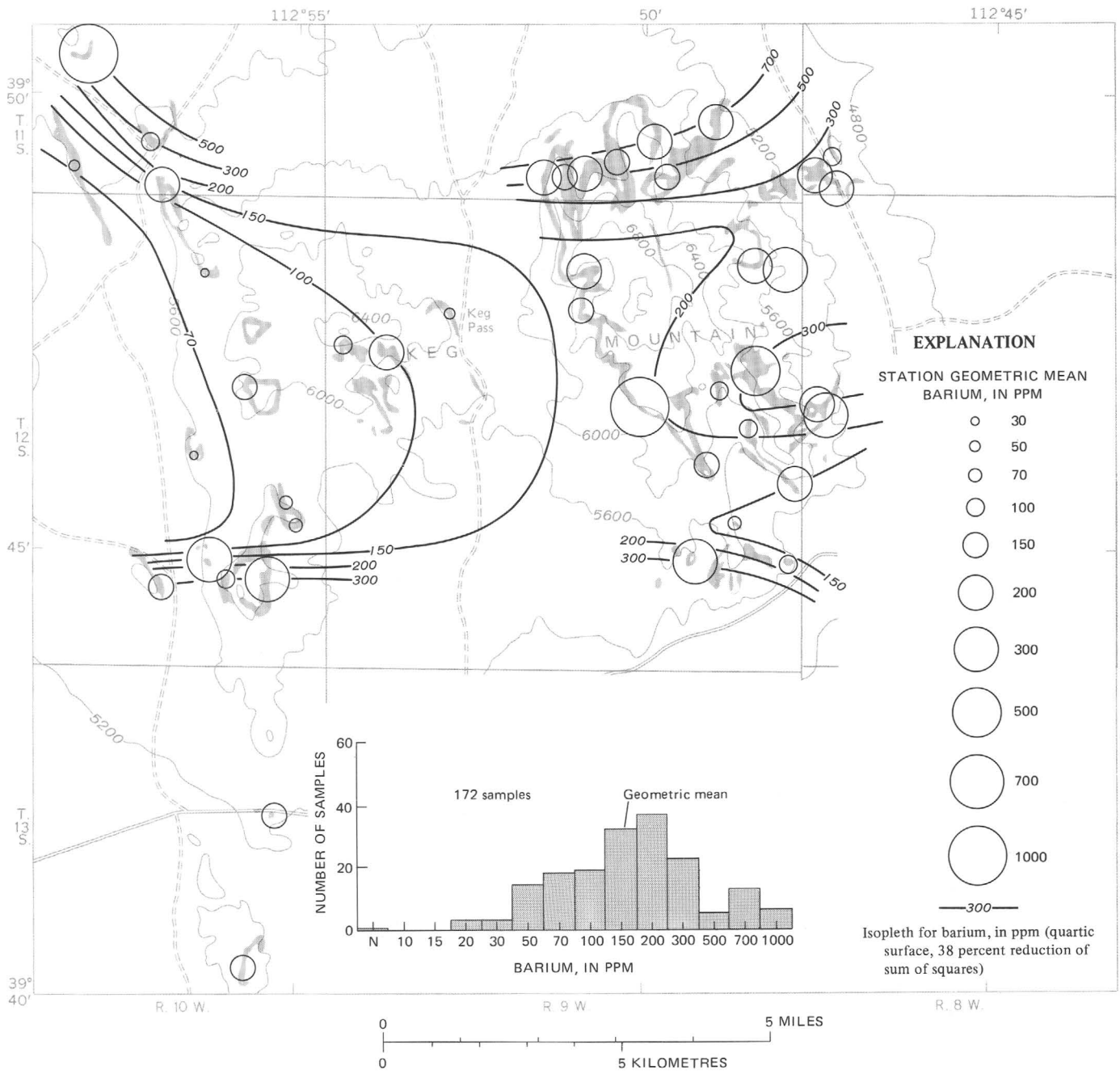

FIGURE 11. — Barium content of water-laid tuff in the Keg Mountain area.

(Lindsey, 1975), suggesting that a mineralization factor, if present, operated only at a very weak intensity.

R-MODE FACTOR ANALYSIS

Petrogenetic parameters (α's, F's) in the model may be defined by a method known as R-mode factor analysis; detailed discussions of factor analysis were presented by Harman (1960), Cooley and Lohnes (1962, p. 151–172) and Miesch, Chao, and Cuttitta (1966). The method was used to develop a model which would account for the variation of physical properties, mineralogy, and chemical composition observed in water-laid tuffs of the Thomas Range (Lindsey, 1975), and the account in that report is repeated here. The method involves four major steps:

1. An $m \times m$ correlation matrix (R-matrix) is computed, where m is the number of measured variables.
2. The R-matrix is solved for m roots (eigenvalues) and the number of large roots (p) is selected as the minimum number necessary to account for a major part of the total variance in the system.
3. A provisional coefficient matrix (the factor

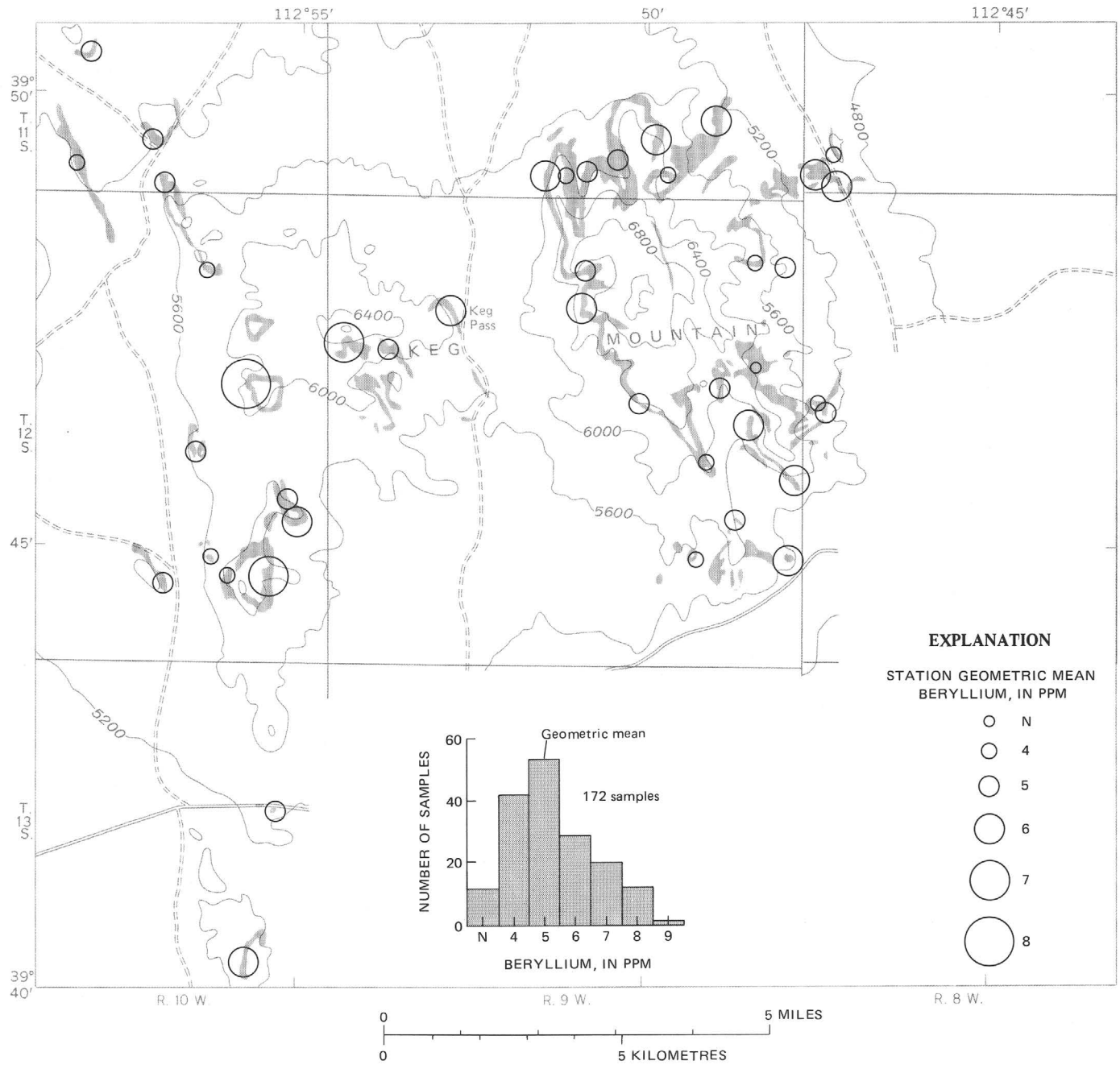

FIGURE 12. — Beryllium content of water-laid tuff in the Keg Mountain area.

loadings) used to define the principal components is computed.

4. A final coefficient matrix defined by the Varimax criterion (Harman, 1960, p. 301) is derived from the factor-loadings matrix. The Varimax loadings are arbitrarily accepted as the α-coefficients in the model.

The data matrix, x_{ij}, is N by m in size where N is the number of samples and m is the number of variables. The degree of linear association between two variables j and k is measured by the correlation coefficient:

$$r_{jk}=\frac{s_{jk}}{\sqrt{s_j^2 s_k^2}},$$

where s_{jk}, the covariance, is computed by

$$s_{jk}=\frac{\sum_{i=1}^{N} x_{ij}x_{ik}}{N}-\bar{x}_j\bar{x}_k,$$

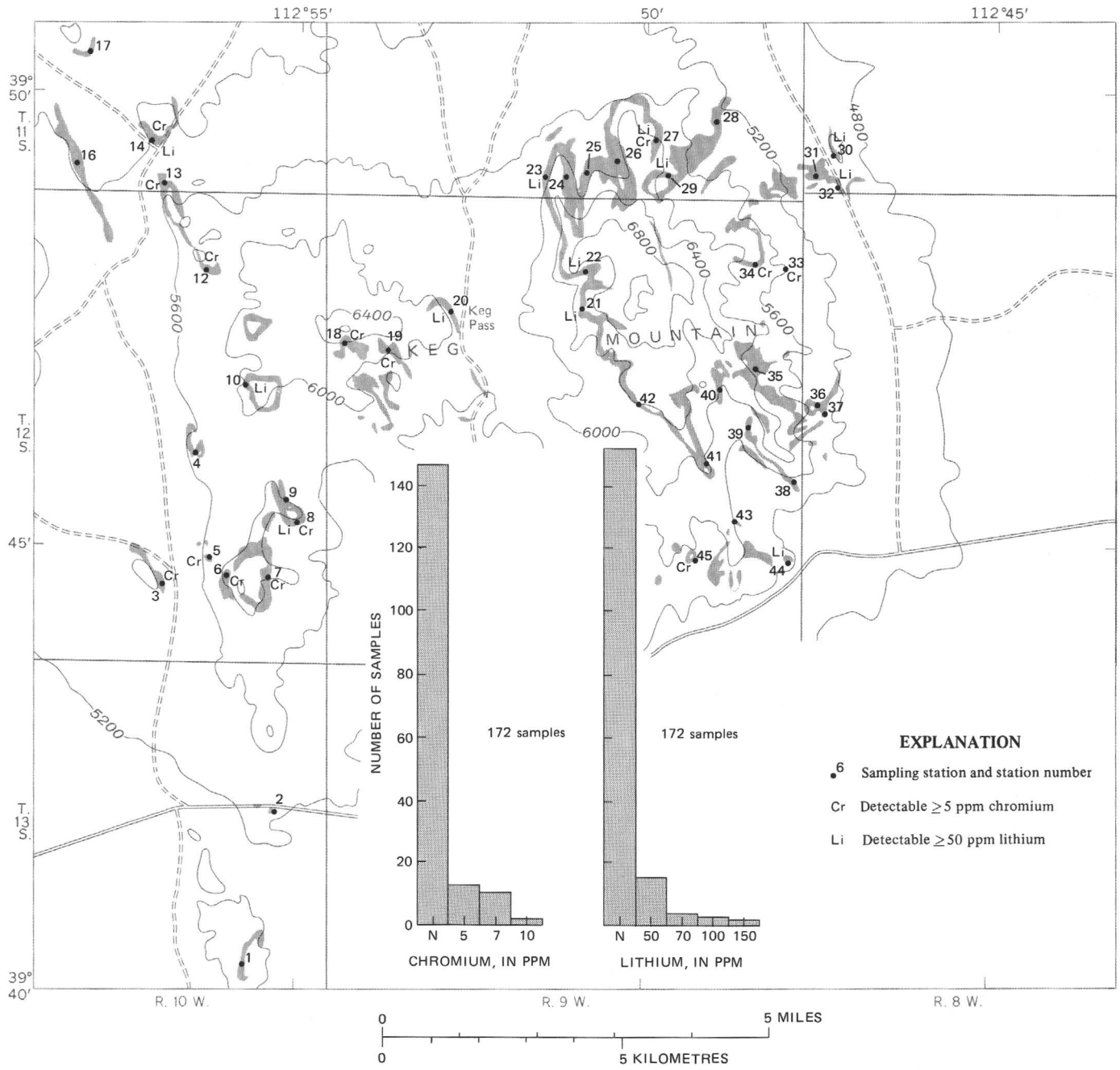

FIGURE 13. — Chromium and lithium content of water-laid tuff in the Keg Mountain area.

and s_j^2, the variance, is computed by

$$s_j^2 = \frac{\sum_{i=1}^{N} x_{ij}^2}{N} - \bar{x}_j^2.$$

Linear covariation between the variables is expressed by the $m \times m$ matrix of correlation coefficients, or R-matrix. A correlation coefficient of $r = 1.0$ indicates perfect linear interdependence, $r = 0$ indicates no linear dependence, and $r = -1.0$ indicates perfect inverse linear dependence. Because the genetic significance of the correlation coefficients is subject to the restrictions of closure, the correlation coefficients between the petrologic variables in this study must be viewed as descriptive measures of covariation.

Factor analysis commonly begins with principal components extraction. Such analysis may be understood in terms of m-dimensional space, where m is the number of

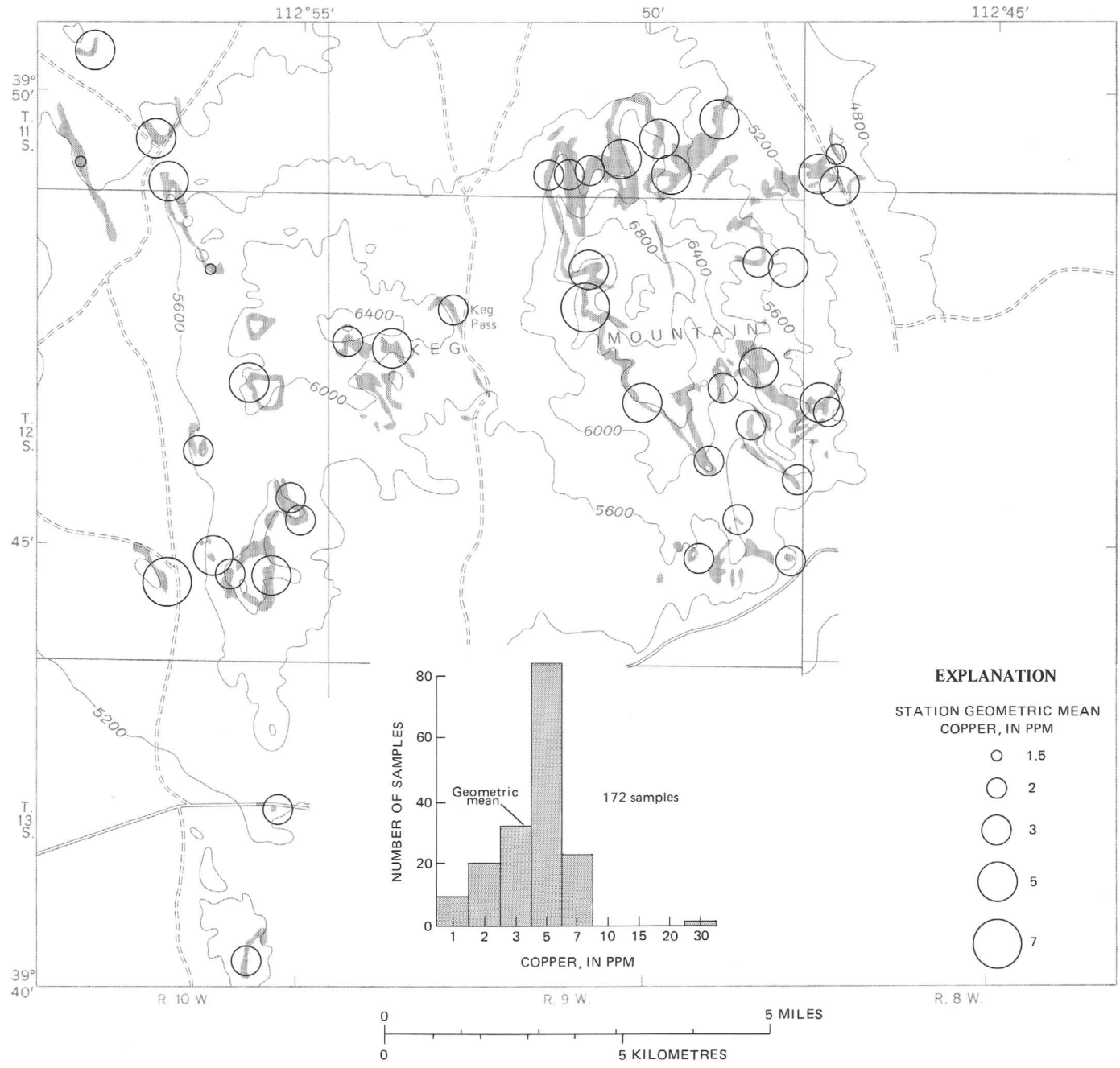

FIGURE 14. — Copper content of water-laid tuff in the Keg Mountain area.

original variables. Each variable defines a dimension in the m-space and the position of each of N samples can be plotted in terms of the m coordinates. Presumably the N samples will tend to cluster as an elongate swarm of points in the m-space. The object of the principal component analysis is to find new uncorrelated variables which measure what the original variables have in common and which produce a maximum variance among samples. The first principal component is located along the major axis of the sample cluster so that the sample projections onto it are maximized. This axis is a new variable which describes the largest possible proportion of the variance. A second axis is located at right angles to the first so that the next largest proportion of variance is explained, and so on. As many as m axes are possible, but some number $p<m$ will commonly account for most of the variance. The variances of the principal components are equal to their eigenvalues. The principal components, following standardization to unit variance, are related to original variables by a new set of coefficients, the factor loadings.

If some number $p<m$ axes accounts for most of the

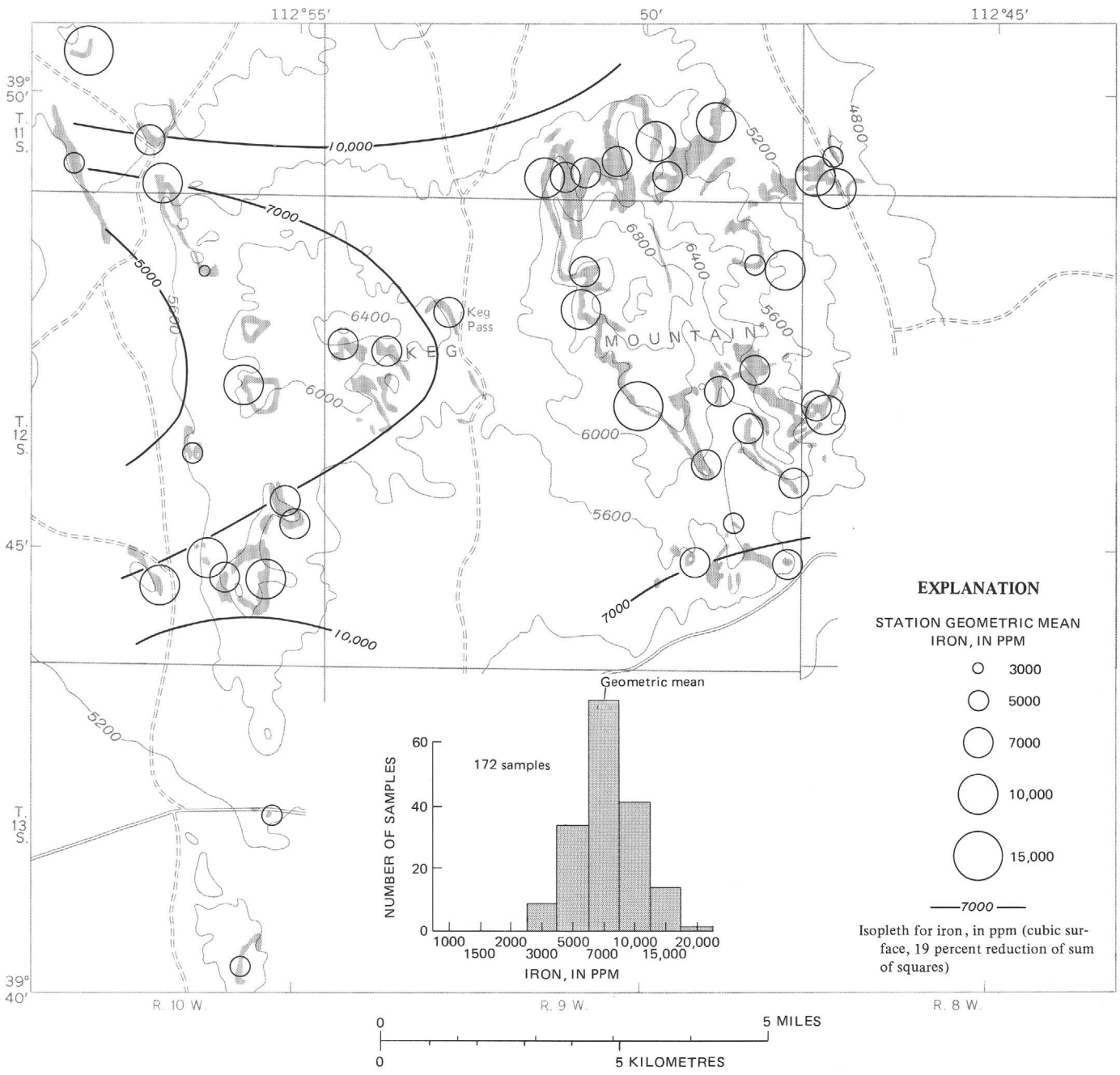

FIGURE 15. — Iron content of water-laid tuff in the Keg Mountain area.

variance (that is, the N points occur largely in p-dimensional space), it is often desirable to rotate the p axes so that they may be more readily interpreted. Rotation may be done in any manner which facilitates interpretation, but the most commonly used objective method of rotation utilizes the Varimax criterion (Harman, 1960, p. 301). The Varimax criterion requires that the variance of the squared factor loadings be maximized and this tends to simplify the resulting factors by yielding large positive or negative loadings for only a few variables on each factor. The rest of the loadings in each factor tend to be near zero. The resulting close association of a few variables with the Varimax factors will allow them to be more readily interpreted. The Varimax loadings specify the relationship of the original variables to the Varimax axes (factors); the axes may be used as a reference system to plot the original variables as vectors. If the sum of the first p eigenvalues of the R-matrix approaches m, the cosines of the angles between vectors in the p-space will approximate the original correlation coefficients.

Because only $p<m$ axes are retained in the model, less

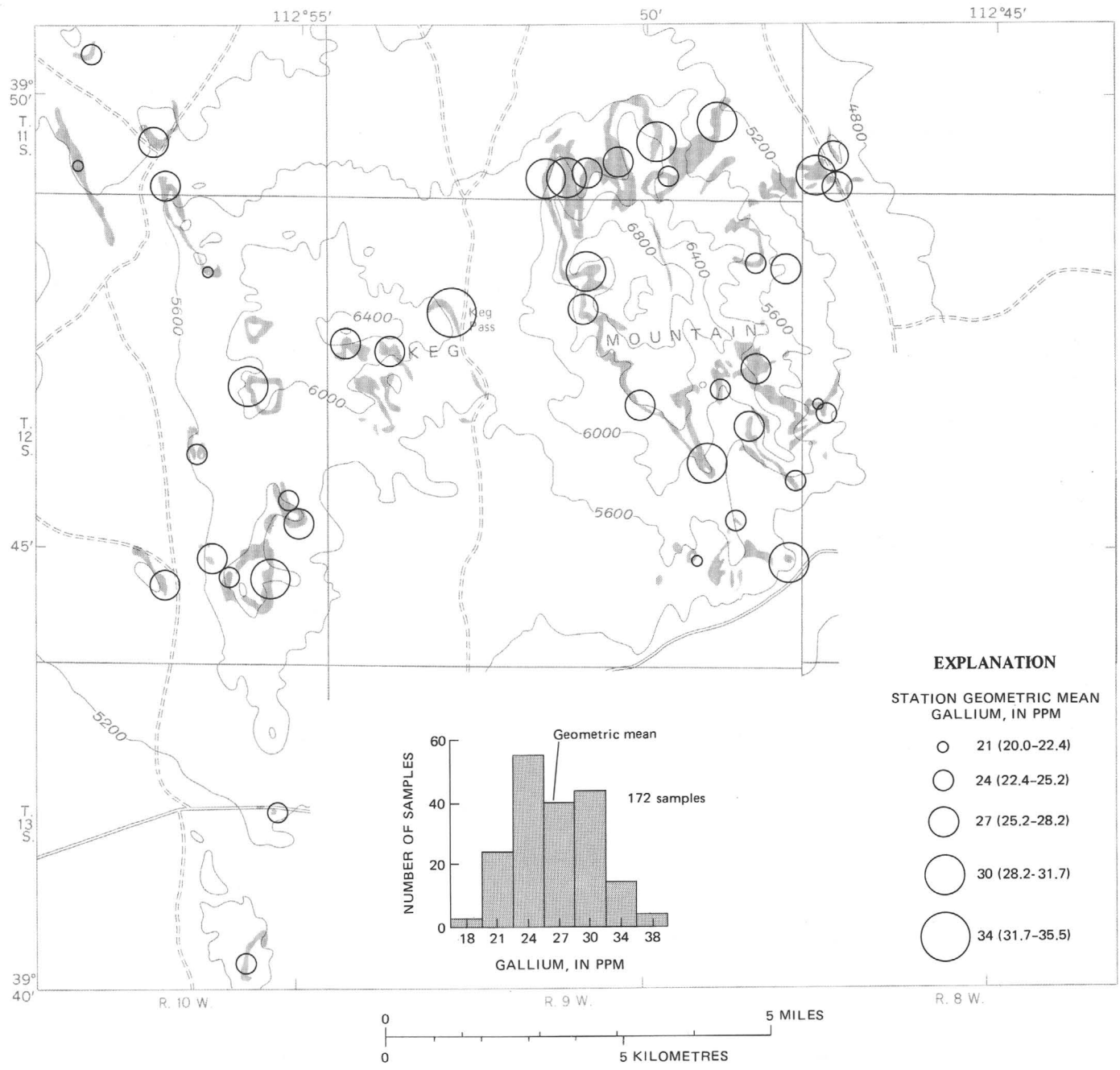

FIGURE 16. — Gallium content of water-laid tuff in the Keg Mountain area.

than 100 percent of the total variance will be explained. The proportion of variance explained for each variable in the factor solution is termed its "communality" (h^2). Geometrically, the square of the vector length of the original variable plotted in the p-space of the factor solution will be h^2. The remaining, unexplained variance ($1-h^2$) is termed the unique component; it consists of unrecognized factors and laboratory error.

FACTOR ANALYSES OF THE WATER-LAID TUFF DATA

Correlation coefficients were calculated between all minerals and trace elements for which more than 30 percent of the data was above the detection limit (table 5). In addition, the variable "glass" was included because it proved to be helpful in the interpretation. All other variables were not included in the analysis because their frequency distributions were more than 30 percent censored. As before, a log transformation was made on all variables except Nb and eU prior to calculation of the R-matrix.

A principal components analysis of the data was then performed on a 19×19 R-matrix with unities in the

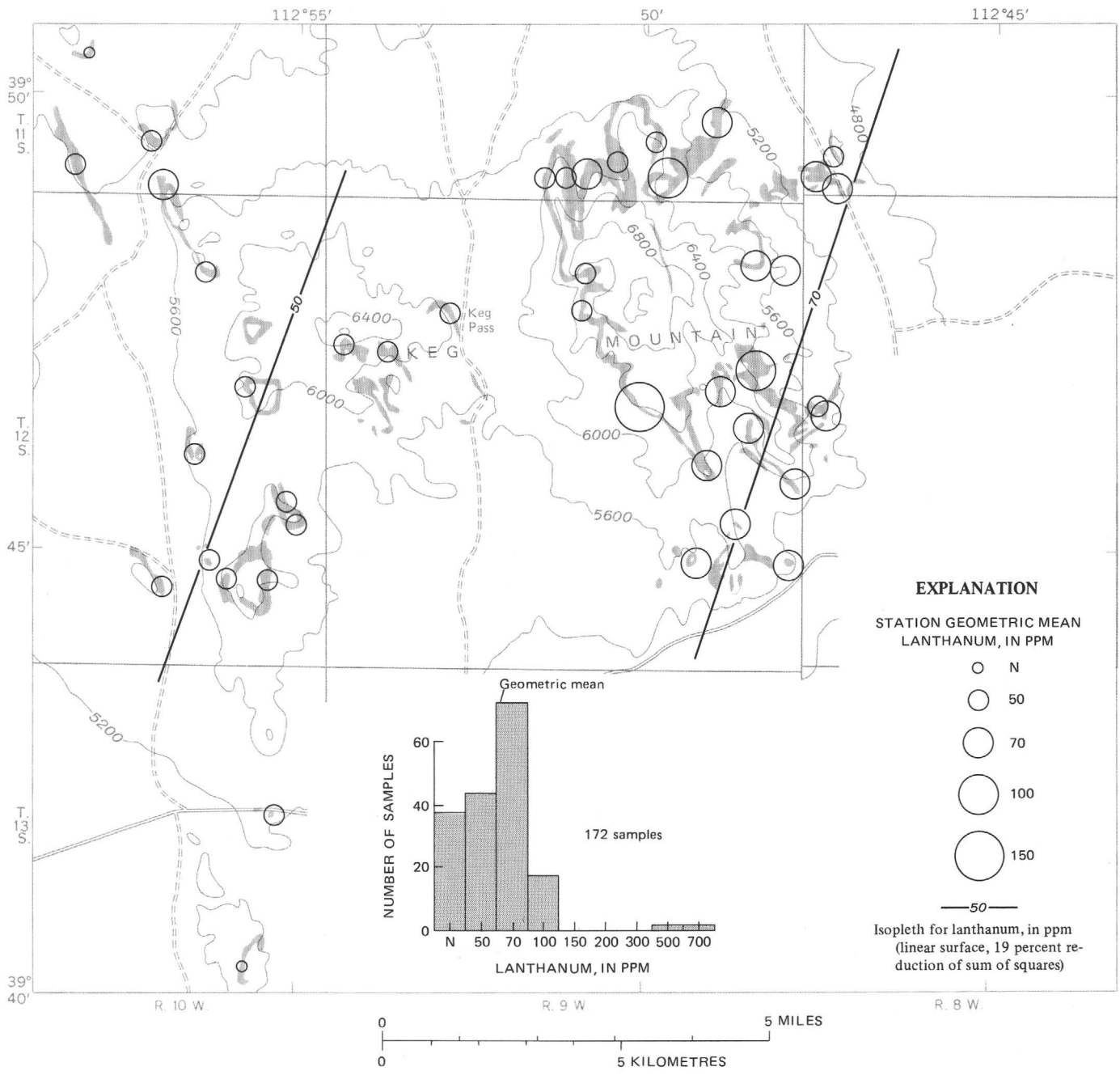

FIGURE 17. — Lanthanum content of water-laid tuff in the Keg Mountain area.

diagonal. The p largest principal components to be preserved for rotation and interpretation were selected by examining the magnitude of the eigenvalues and the communalities for various solutions. The eigenvalues, which measure the proportion of the total variance explained by each principal component, are plotted in figure 27 for the 10 largest principal components (factors). Visible declines occur after the second and sixth eigenvalues, suggesting that from two to six principal components might be considered for rotation. Various experiments were conducted by Varimax rotation of two through six axes and the communalities of all variables for each solution were compared (table 6) with the percentage of nonerror variance as estimated in table 3. Study of the communalities for each solution led to selection of a five-factor model as the most suitable choice. Communalities of some elements (La, Nb, and Zr) already exceed the nonerror variance in the three-factor model, but the communalities for many other variables (α-cristobalite, potassium feldspar, Be, Pb, and Sr) remain quite low until four or five components are rotated. When six components are rotated, the com-

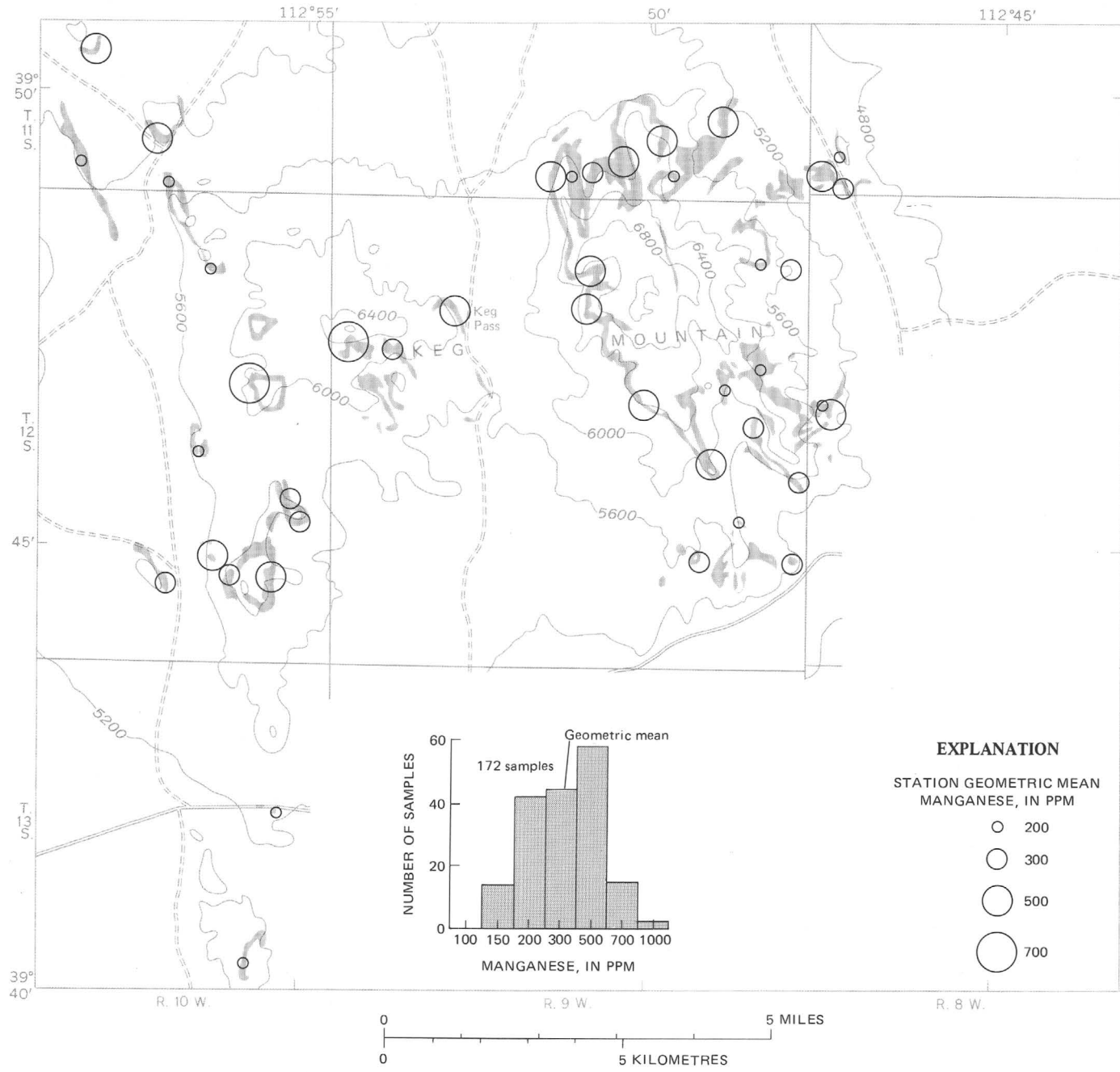

FIGURE 18. — Manganese content of water-laid tuff in the Keg Mountain area.

munalities of 10 elements exceed the nonerror variance; the increase of the communality for eU from 36 to 68 percent in the face of only 35 percent "real" or nonerror variance indicates that the six-factor solution is "explaining" variance in eU that is actually error in large part. The five-factor model appears to be more desirable than the four-factor model; the communalities of α-cristobalite and potassium feldspar are much higher in the five-factor model; other communalities are likewise improved while the number of elements with excessively high communalities does not increase. The excessively high communality of Zr throughout all experiments is bothersome, although as will be shown shortly, the location of Zr with respect to the factor axes results in a reasonable interpretation. The five-factor model accounts for 72 percent of the total variance in the normalized data.

The five principal components were rotated by the Varimax method and the loadings of each variable on the five Varimax factors are shown in table 7; the Varimax loadings may be accepted as the α-coefficients of the petrogenetic model. Each factor (F_1, F_2 . . . F_p)

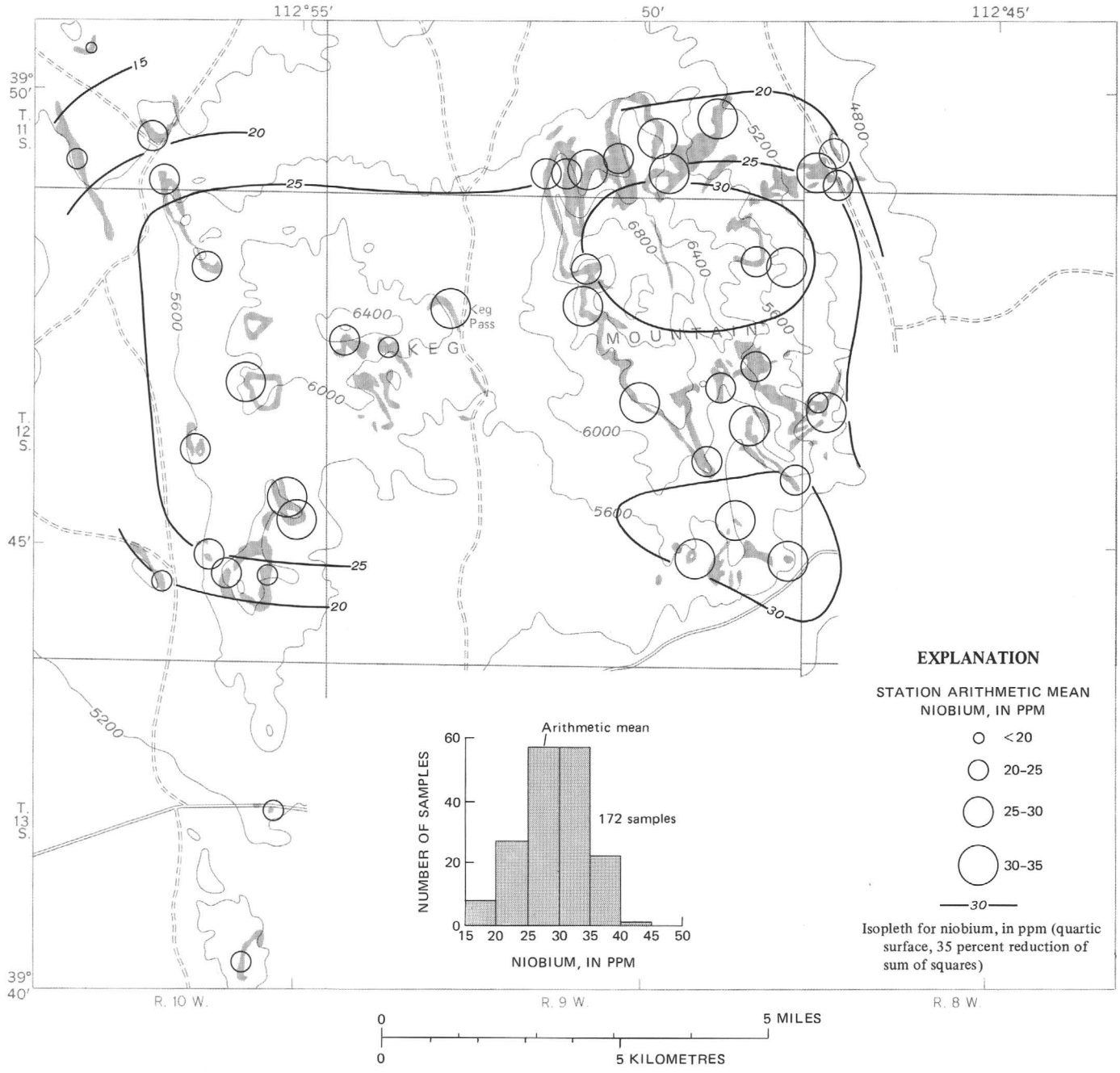

FIGURE 19. — Niobium content of water-laid tuff in the Keg Mountain area.

can be interpreted from the association of variables which load most heavily on it. The factor interpretations are as follows:

Factor I (F_1): Concentration of major detrital minerals. Barium, Fe, V, Ti, Cu, and quartz, and to a lesser extent Mn, Zr, and potassium feldspar have high positive loadings on factor I.

Factor II (F_2): Initial diagenesis (zeolitization). Clinoptilolite and Sr have high positive loadings; glass and to a lesser extent eU have negative loadings.

Factor III (F_3): Concentration of minor rare earth-bearing detrital minerals. Lanthanum, Nb, Y, and Zr have positive loadings on factor III.

Factor IV (F_4): Late magmatic concentration of trace elements(?). Lead, Ga, Be, and to a lesser extent Mn and Nb have positive loadings on factor IV.

Factor V (F_5): Advanced diagenesis (feldspathization). Cristobalite and potassium feldspar have positive loadings on factor V.

Factor I, representing concentration of major detrital minerals, clearly reflects the processes of erosion and sedimentation whereby detrital quartz, feldspar, and

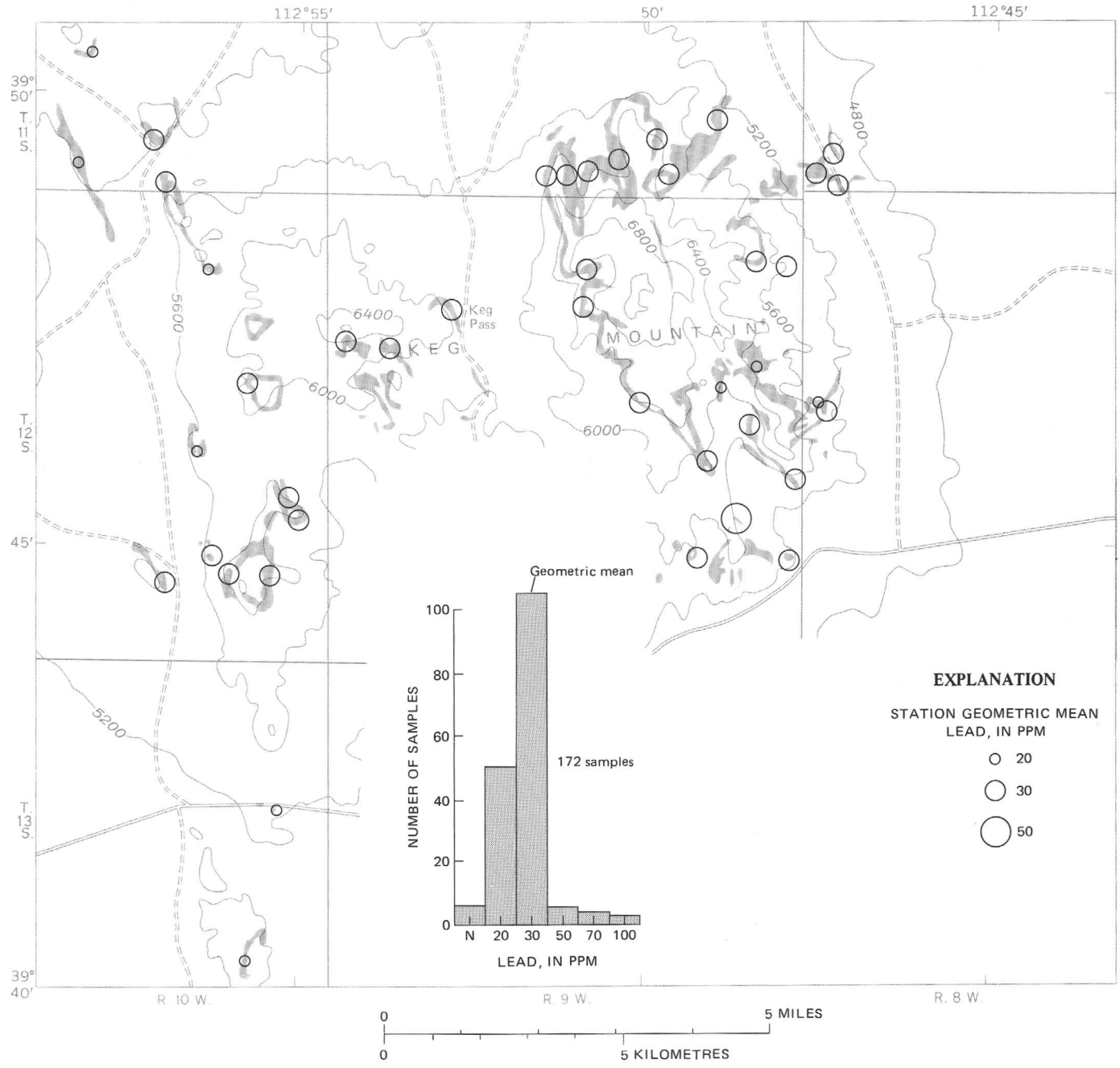

FIGURE 20. — Lead content of water-laid tuff in the Keg Mountain area.

iron oxides are concentrated to form the detrital facies described earlier. Tuff samples which have high concentrations of quartz, potassium feldspar, Ba, Cu, Fe, Mn, V, Ti, and Zr and thus would be expected to score high on factor I include those of the detrital facies. These trace elements are abundant in many samples, indicating that the influence of detrital processes in the water-laid tuff was widespread.

The association of trace elements with factor I is probably due to substitution of some of these elements (Mn, Ti, and V) in magnetite (Deer, Howie, and Zussman, 1962, v. 5, p. 68–77). As much as 2 percent magnetite and hematite was recovered from samples with high concentrations of factor I trace elements. Perhaps some of the trace elements are also present in unusually large amounts of other minerals, such as feldspar, barite, and zircon. No barite has been identified in heavy mineral separates, however, and it seems more likely that Ba may reside in detrital plagioclase. Concentrates of magnetite and hematite from tuff sam-

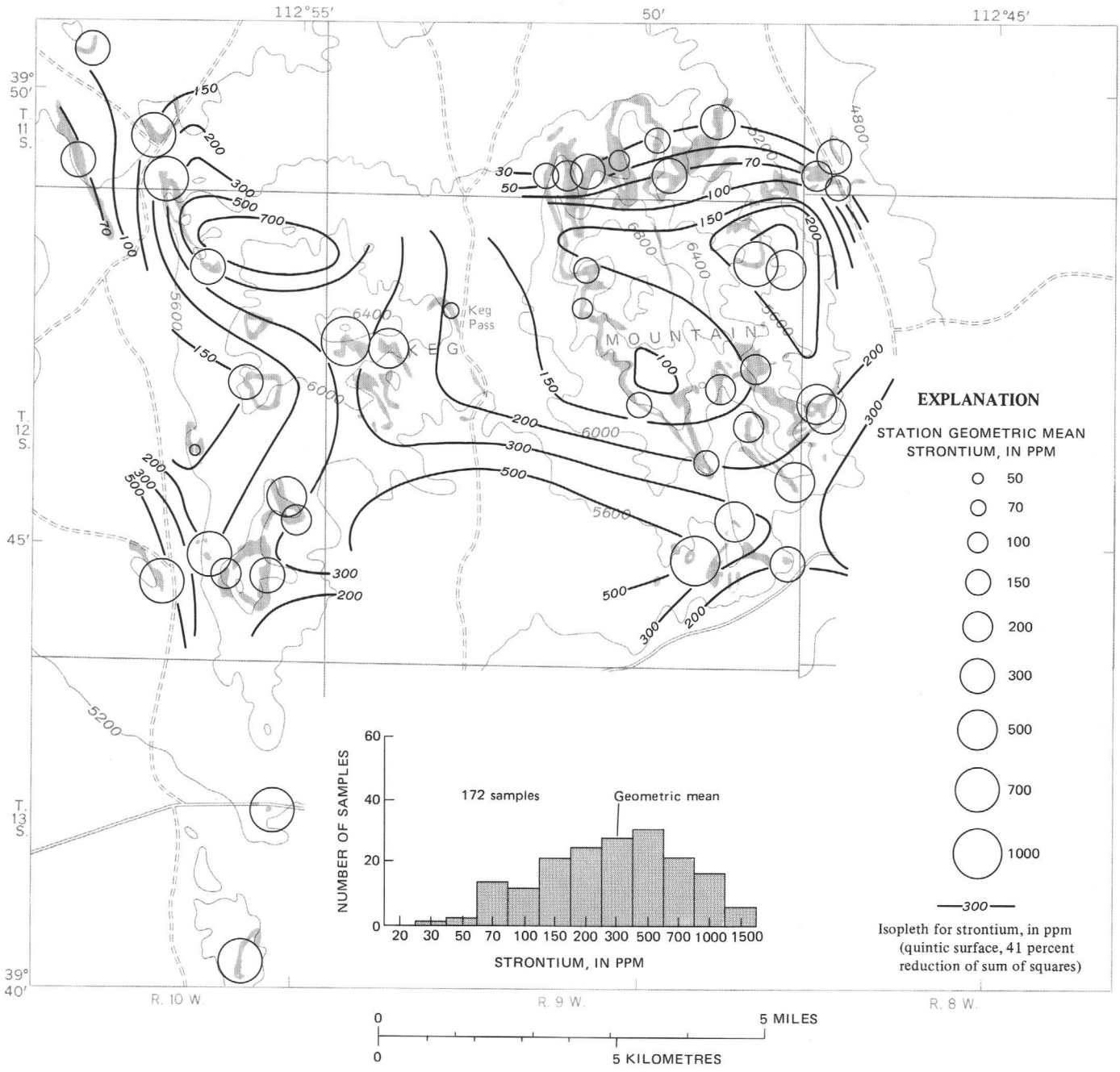

FIGURE 21. — Strontium content of water-laid tuff in the Keg Mountain area.

ples rich in these minerals were analyzed by spectrographic methods to determine the extent of association of factor I trace elements with the iron oxides. High concentrations of Co (as much as 50 ppm), Cr (as much as 200 ppm), Cu (7–15 ppm), Mn (3,000 ppm), Ti (7,000–15,000 ppm), V (300–500 ppm), and Zn (700 ppm) were found in four magnetite concentrates. A single concentrate of hematite showed generally lower concentrations of these elements, except Cu and Zn, which showed the same degree of concentration as in magnetite. These results indicate that the high loadings of Cu, Mn, Ti, and V on factor I are due in part to their presence in magnetite. Given sufficiently sensitive analytical methods, the elements Co, Cr, and Zn might also be expected to associate with factor I.

Factor II, the factor for initial diagenesis (zeolitization), involves the alteration of glass to clinoptilolite and accounts for the widespread distribution of the zeolitic facies in the tuff. The inverse relationship between glass and zeolite in factor II illustrates the effect of closure,

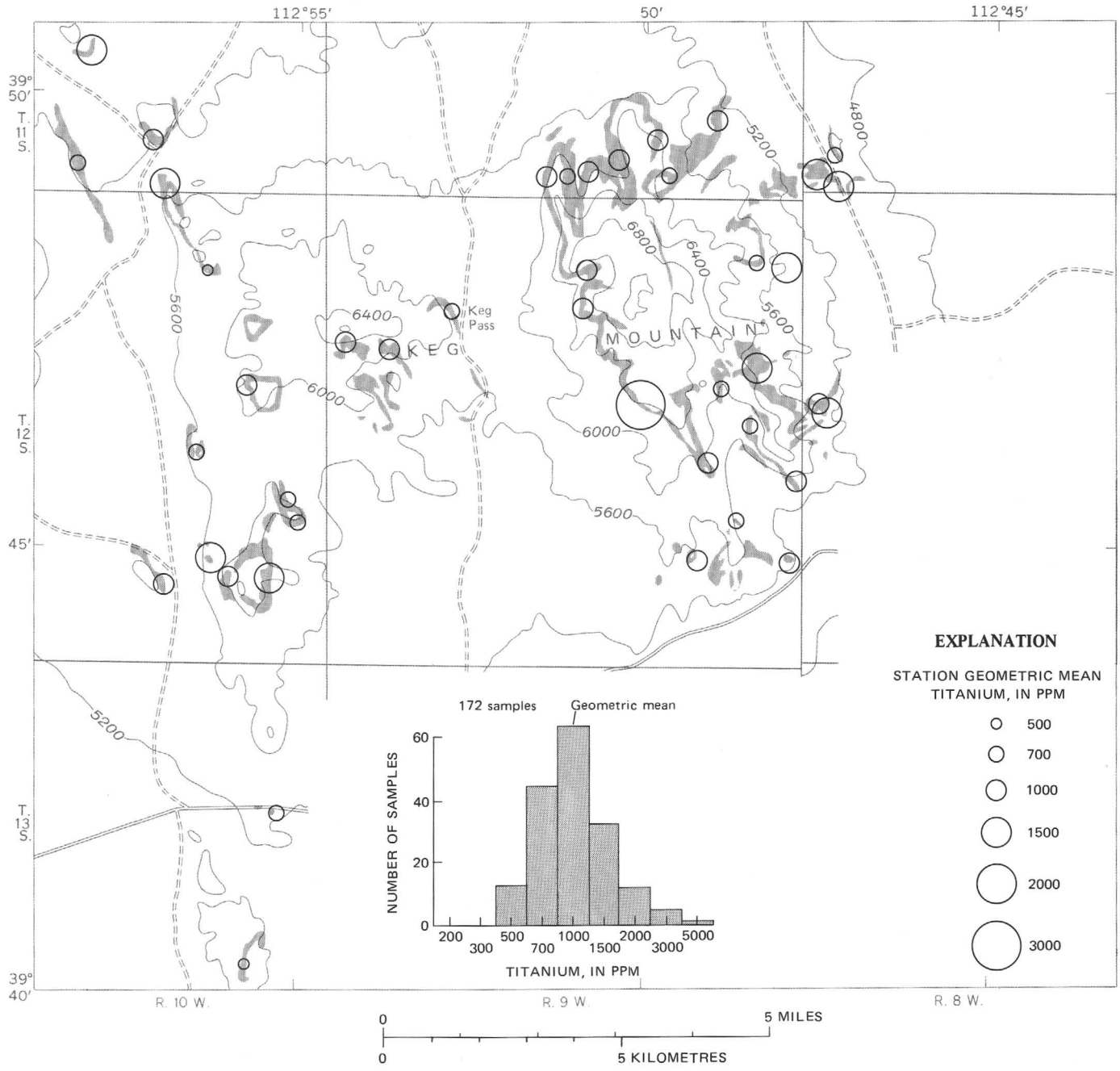

FIGURE 22. — Titanium content of water-laid tuff in the Keg Mountain area.

but nevertheless is understandable in that it corresponds to the alteration of vitric to zeolitic tuff. The relative concentrations of Sr and U (as eU) in the tuff were increased and decreased respectively as zeolitization occurred.

Factor III is interpreted as the concentration of minor detrital minerals. The association of the trace elements La, Nb, Y, and Zr with factor III indicates that the concentration process involves selection of rare earth-bearing minerals. Mineral separates were prepared from tuff samples which contained high concentrations of these elements and sphene and zircon were found to be abundant relative to other tuff samples. Substitution of numerous elements, including rare earths, in sphene has been reported (Deer and others, 1962, v. 1, p. 69–76). Spectrographic analyses of two sphene concentrates show high concentrations of La (1,500–3,000 ppm), Nb (500–1,500 ppm), Ti (>2 percent), and Y (1,500–7,000 ppm). Other rare earths were also found, including Ce (3,000–7,000 ppm), Dy (300–1,500 ppm), Er (150–1,000 ppm), Gd (300–1,500 ppm), Ho (70–300 ppm), Lu (as much as 70 ppm), Nd (3,000–7,000 ppm), Pr (500–2,000

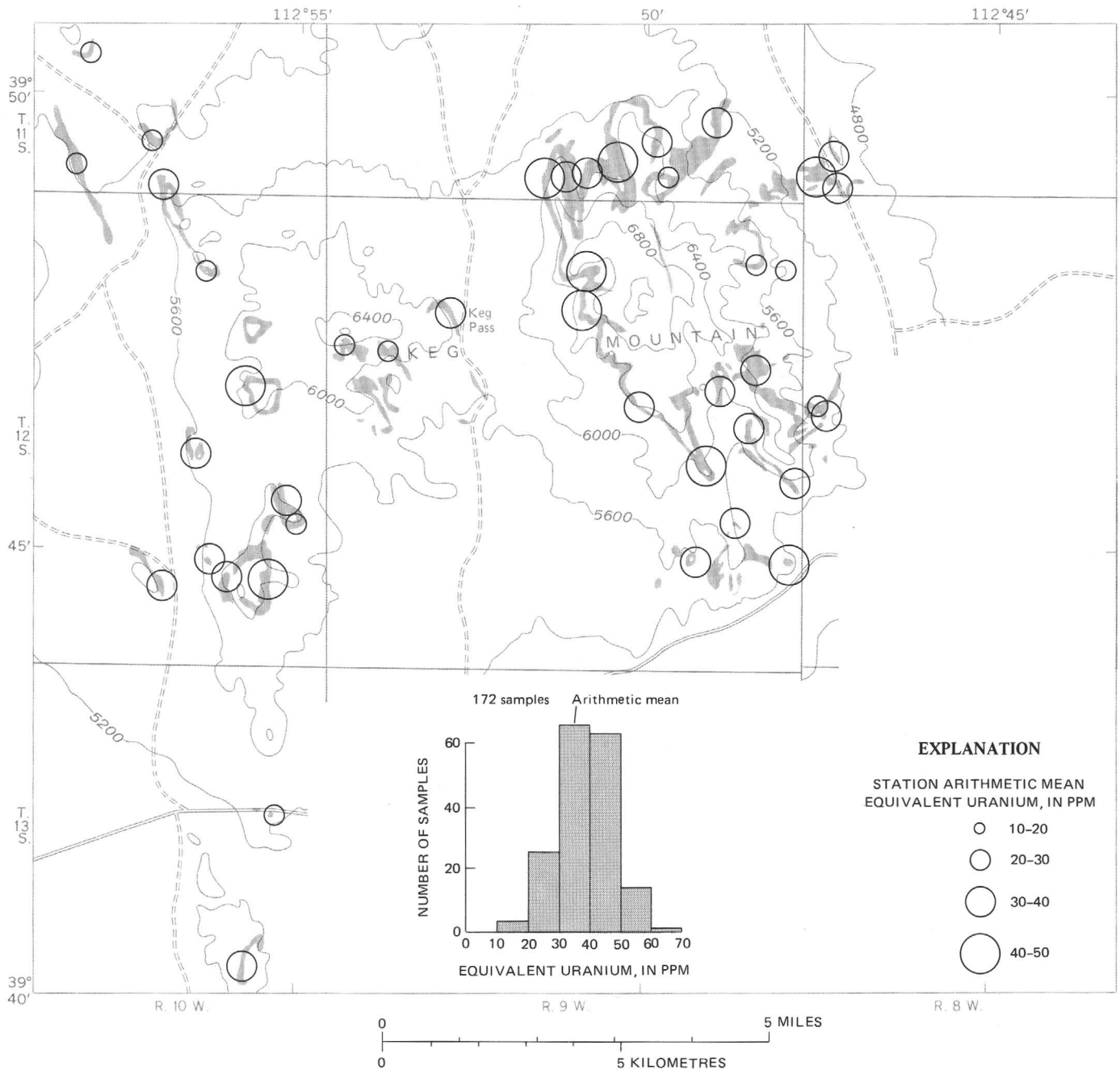

FIGURE 23. — Equivalent uranium content of water-laid tuff in the Keg Mountain area.

ppm), Sm (700–2,000 ppm), Tm (as much as 100 ppm), and Yb (150–500 ppm); these elements were not included in the direct reading spectrographic analysis of the tuff samples. These results confirm that the high loading of La, Nb, Y, and Zr on factor III is due in part to the concentration of sphene and zircon.

Heavy minerals in the underlying volcanic rocks were examined also, in order to determine which rock units might be likely sources of the sphene and zircon. Abundant sphene was recovered from rhyolitic welded ash-flow tuff in the central part of the Keg Mountain area, and abundant pink zircon, similar to some observed in the water-laid tuff, was recovered from the rhyolite of Keg Mountain in the southeastern part of the area. These rock units underlie the tuff throughout the eastern half of the Keg Mountain area and could be the source of the easterly concentration of the trace elements La, Nb, Y, and Zr.

Another aspect of interpretation is the possibility of systematic laboratory error among the trace elements associated with factor III. The communalities of La, Nb, and Zr are all substantially in excess of the nonerror

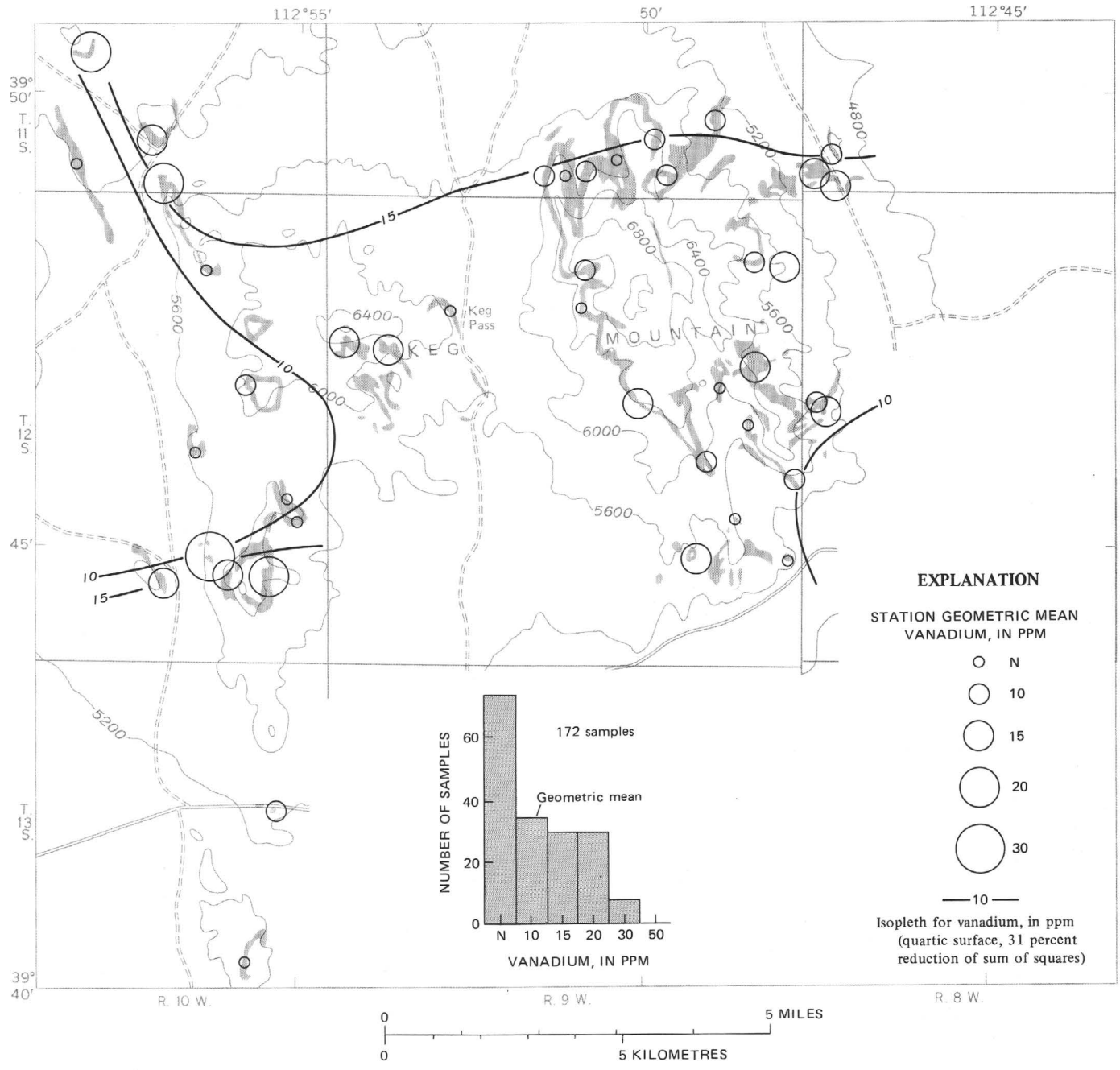

FIGURE 24. — Vanadium content of water-laid tuff in the Keg Mountain area.

variance (table 6), indicating that factor III "explains" considerable error. The specific cause of laboratory error is unknown. The fact that Y is also included among the trace elements associated with factor III (the communality of Y does not exceed the nonerror variance) and that all of these elements show similar geographic trends indicates that the association is real and not merely an artifact.

Factor IV is the most difficult to interpret. The high positive loadings of Ga and Be, and to a lesser extent Mn and Nb, at once suggest that factor IV represents the effect of beryllium mineralization on the tuff. Lead was not concentrated by mineralization of tuff in the Thomas Range (Lindsey, 1975), however, and its high loading on factor IV suggests that some process other than beryllium mineralization is responsible. Another feature of tuff near areas of beryllium mineralization is the high degree of skewness shown by the frequency distribution for beryllium; nearly half of the samples of tuff that were studied from the Thomas Range contain 10 ppm or more Be and a few samples were found to contain more than 100 ppm Be (Lindsey, 1975). In contrast, the berllium

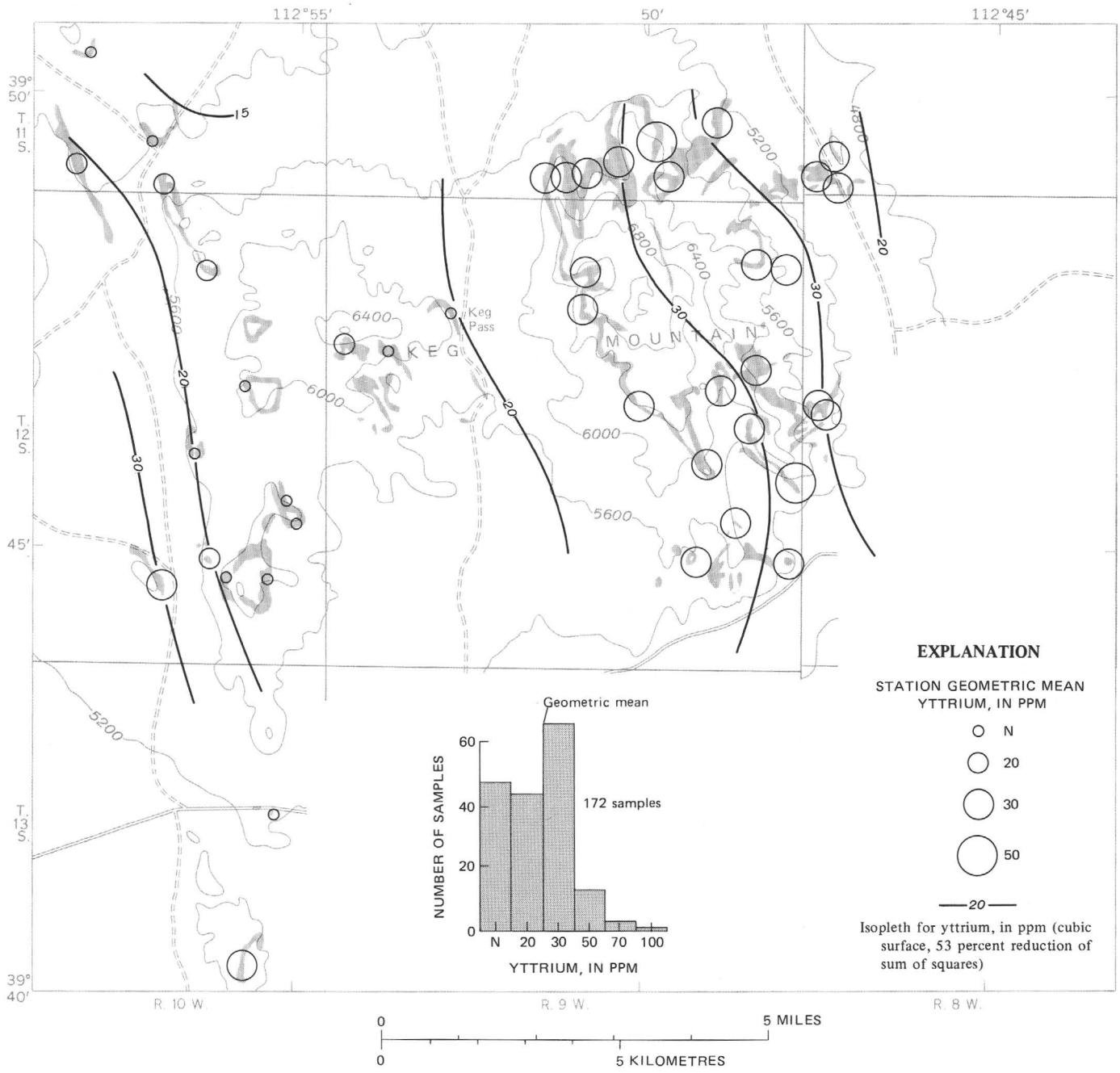

FIGURE 25. — Yttrium content of water-laid tuff in the Keg Mountain area.

concentration in water-laid tuff of the Keg Mountain area never exceeds 10 ppm and the frequency distribution for Be is skewed very little (fig. 12). Hence comparison of frequency distributions for beryllium indicates that effects of beryllium mineralization at Keg Mountain are weak or absent.

An alternative interpretation of factor IV is that it represents concentration of trace elements in the original rhyolite magma. The rhyolites of the Thomas Range, which might approximate the composition of the original magma, are well known for the occurrence of topaz, beryl, and bixbyite in lithophysae (Staatz and Carr, 1964, p. 102–106); these minerals indicate a tendency toward concentration of F, Be, and Mn in the vapor phase of the magma. Spectrographic analyses of rhyolites in the western Utah beryllium belt show a general enrichment of Be (3–20 ppm), Ga (15–50 ppm), Nb (30–100 ppm), Pb (40–60 ppm), and Sn (as much as 50 ppm) (Shawe, 1966, table 3); older, less silicic rocks from the same area usually contain notably less of these elements. Thus the association of Pb-Ga-Be, and to a lesser extent Mn and Nb, could be interpreted as due to

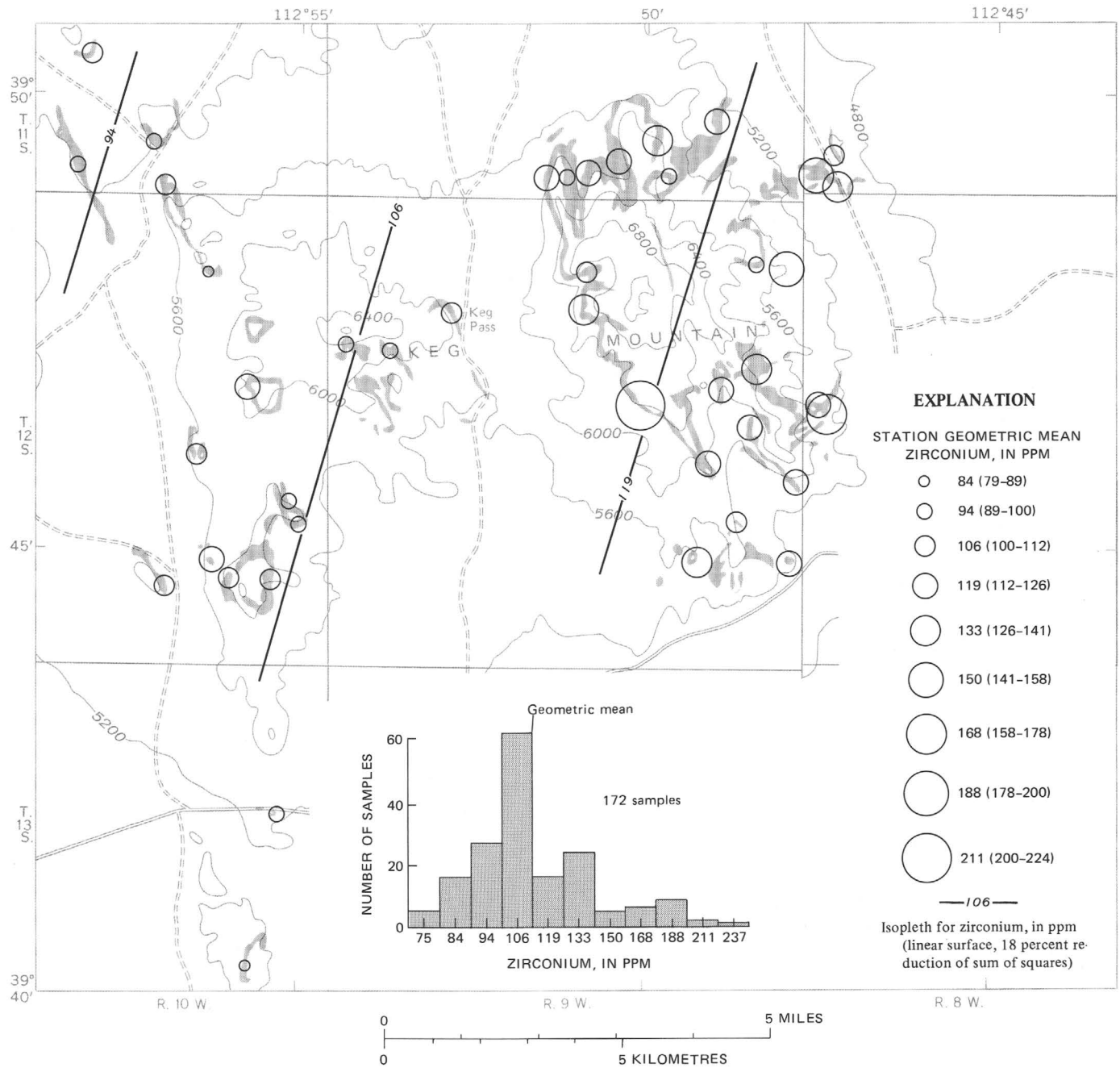

FIGURE 26. — Zirconium content of water-laid tuff in the Keg Mountain area.

concentration in the more silicic, vapor-rich portions of a parent rhyolite magma.

Factor V is the association of cristobalite and potassium feldspar and represents the final stage of diagenesis. The concentration of trace elements was not affected by advanced diagenesis.

CONCLUSIONS

EROSION AND SEDIMENTATION

A petrogenetic model derived by *R*-mode factor analysis of mineral and chemical data shows that concentration of detrital minerals by erosion and sedimentation is the dominant process in controlling the distribution of many metallic elements in the water-laid tuffs of western Utah. Detrital heavy minerals containing Al, Fe, Mg, Mn, Ti, and Zr are concentrated mainly in local areas (1–2 mi, 1.6–3.2 km) of tuff in the southern part of the Thomas Range (Lindsey, 1975). In the Keg Mountain area, a detrital assemblage of heavy minerals containing Fe, Cu, Mn, Ti, V, and Zr is associated with abundant quartz and feldspar derived from older volcanic rocks. This detrital facies also forms local (1–2

TABLE 5. — *Correlation coefficients based on analyses of 172 samples of water-laid tuff from the Keg Mountain area*

	Log quartz	Log α-cristobalite	Log K-feldspar	Log glass	Log Ba	Log Be	Log Cu	Log Fe	Log Ga	Log La	Log Mn	Nb	Log Pb	Log Sr	Log Ti	eU	Log V	Log Y	Log Zr
Log clinoptilolite	−0.22	−0.02	−0.18	−0.78	−0.28	−0.30	−0.21	−0.47	−0.51	−0.13	−0.52	−0.22	−0.17	0.57	−0.35	−0.37	−0.08	−0.19	−0.33
Log quartz		.21	.67	−.15	.61	.13	.37	.60	.16	.05	.38	−.20	−.05	.20	.47	.12	.46	.02	.21
Log α-cristobalite			.40	−.18	.24	.19	.18	.27	.08	.00	.24	.01	−.04	−.13	.23	.00	.21	−.09	.16
Log K-feldspar				−.11	.50	.19	.25	.54	.21	.08	.36	−.01	−.03	.01	.45	.25	.30	.00	.27
Log glass					.02	.29	.12	.20	.50	.03	.34	.28	.24	−.50	.11	.36	−.09	.24	.21
Log Ba						.06	.51	.76	.19	.30	.36	−.06	−.07	.19	.77	.07	.67	.19	.54
Log Be							.34	.38	.53	−.01	.45	.27	.25	−.16	.18	.18	.07	−.02	.13
Log Cu								.58	.41	.19	.37	.13	.16	.07	.48	.16	.50	.13	.32
Log Fe									.47	.34	.65	.16	.14	.00	.88	.30	.72	.10	.64
Log Ga										.20	.53	.38	.47	−.26	.34	.36	.25	.12	.27
Log La											.08	.52	.17	.02	.50	.12	.27	.46	.62
Log Mn												.17	.33	−.15	.51	.34	.43	−.02	.33
Nb													.45	−.13	.23	.24	.00	.45	.44
Log Pb														−.01	.04	.30	.06	.22	.10
Log Sr															.03	−.26	.32	−.02	−.12
Log Ti																.20	.76	.17	.76
eU																	−.02	.24	.24
Log V																		.00	.42
Log Y																			.40

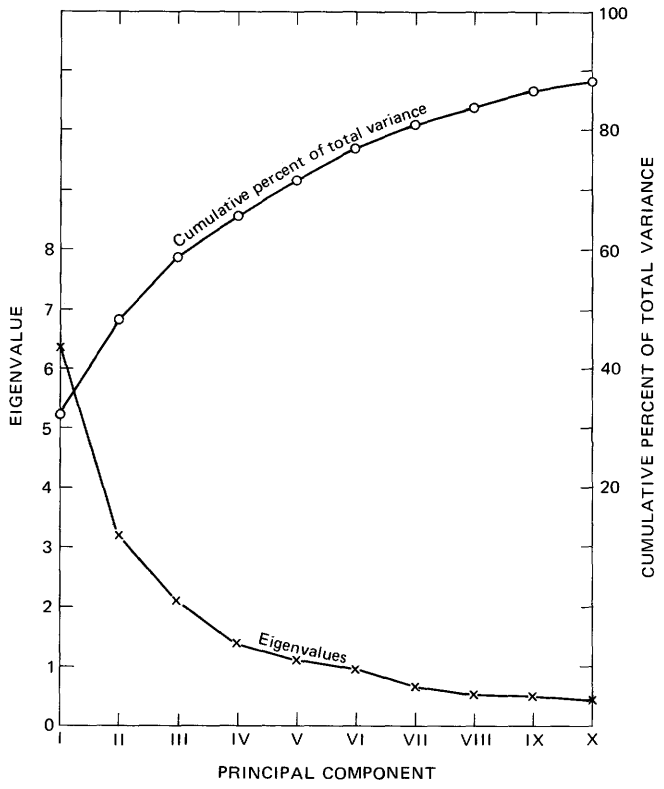

FIGURE 27. — Eigenvalues and cumulative proportion of total variance explained by the first 10 principal components.

mi, 1.6–3.2 km) concentrations in the tuff. A second detrital assemblage consists of the heavy minerals sphene and zircon; these are defined by a regional eastward increase in the abundance of La, Nb, Y, and Zr.

The effects of erosion and sedimentation on concentration of various heavy elements in the water-laid tuffs should pose no threat to defining halo effects of beryllium and fluorite mineralization in tuffs of western Utah. They might present serious problems in geochemical exploration for heavy metal and rare earth deposits, however, and the evaluation of trace element anomalies in tuffs should take into consideration the effect of erosion and sedimentation on trace element concentration.

DIAGENESIS

Diagenetic alteration of the water-laid tuff in the Keg Mountain area was approximately the same type as that which affected the tuff in the Thomas Range. Factor analysis of mineral and chemical data showed that three stages of diagenetic alteration could be distinguished in tuff of the Thomas Range (Lindsey, 1975). The initial stage involved alteration of glass to clinoptilolite, accompanied by relative loss of alkalis, (Na_2O, K_2O, and Rb) eU, F, and Mn, and relative gain of Sr and MgO. The second stage involved formation of additional clinoptilolite as well as potassium feldspar and quartz. The concentra-

TABLE 6. — *Communalities (in percent) for two-, three-, four-, five-, and six-factor Varimax solutions, compared to the percent of nonerror variance*

[Italic numbers indicate communalities which exceed the nonerror variance]

	Number of rotated factors					Nonerror variance
	2	3	4	5	6	
Log clinoptilolite	60	68	84	87	87	>99
Log quartz	57	64	64	64	79	85
Log α-cristobalite	15	22	22	70	79	96
Log K-feldspar	43	50	51	69	82	86
Log glass	66	69	76	86	87	96
Log Ba	76	76	81	84	84	95
Log Be	27	41	*58*	*60*	*64*	57
Log Cu	42	42	*49*	*53*	*56*	42
Log Fe	90	91	91	*92*	*92*	91
Log Ga	59	63	*72*	72	*73*	66
Log La	22	*72*	*73*	*75*	*75*	58
Log Mn	52	66	68	69	69	83
Nb	41	*65*	*71*	*79*	*80*	59
Log Pb	29	30	66	66	71	82
Log Sr	38	48	72	78	82	97
Log Ti	82	86	*88*	*88*	*90*	86
eU	33	34	34	*36*	*68*	35
Log V	68	69	71	78	82	93
Log Y	17	54	*56*	*56*	*65*	54
Log Zr	*52*	*71*	*77*	*79*	*81*	47

TABLE 7. — *A five-factor petrogenetic model for the water-laid tuff as defined by the Varimax loadings*

[Coefficients ≤ −0.50 or ≥0.50 are shown in italic type]

Variable	Factors				
	I	II	III	IV	V
Log Mn	*0.51*	−.36	−0.07	*0.50*	0.17
Log Cu	*.61*	.00	.05	.38	−.01
Log quartz	*.71*	.01	−.17	−.01	.32
Log Ti	*.83*	−.13	.38	.04	.14
Log V	*.84*	.20	.08	.11	−.01
Log Fe	*.85*	−.22	.17	.23	.20
Log Ba	*.88*	−.04	.16	−.12	.11
Log clinoptilolite	−.28	*.87*	−.08	−.15	.04
Log Sr	.27	*.80*	−.04	.01	−.22
eU	.06	−.45	.20	.29	.13
Log glass	.01	−*.82*	.09	.26	−.33
Log La	.24	.03	*.82*	.02	.00
Nb	−.13	−.10	*.72*	.47	.04
Log Y	.02	−.13	*.72*	.01	−.13
Log Zr	.49	−.22	*.68*	.00	.14
Log Pb	−.05	.00	.24	*.76*	−.12
Log Ga	.27	−.39	.10	*.69*	.00
Log Be	.12	−.21	−.10	*.68*	.21
Log α-cristobalite	.13	.03	−.01	.07	*.82*
Log K-feldspar	.48	.08	−.02	.02	*.66*

tion of Na_20 and Pb declined while that of Ba and Cr increased. The advanced stage of diagenesis was characterized by the formation of α-cristobalite and additional potassium feldspar with no further chemical change. Bulk density increased and porosity decreased as diagenesis proceeded, and so the final product is a dense tuff composed mainly of potassium feldspar and cristobalite. The three stages of diagenesis probably represent a continuum that results from the action of ground water. Leaching of alkalis from glass results in an ever increasing ratio of alkali/hydrogen ion concentrations as ground water percolates downward through vitric tuff (Hay, 1963), with the result that first clinoptilolite and then potassium feldspar is formed.

Two stages of diagenetic alteration (zeolitic and feldspathic) are distinguished in the water-laid tuff of the Keg Mountain area. They correspond approximately to the initial and advanced stages of diagenesis identified in tuff of the Thomas Range. Data are not available to record the leaching of alkalis from glass in tuff of the Keg Mountain area, but inasmuch as this mechanism is thought to be responsible for diagenetic alteration, removal of alkalis seems probable. As with the tuff of the Thomas Range, the concentration of uranium (as eU) appears to decline during zeolitization whereas Sr increases. The increase in Sr is probably due to its presence in clinoptilolite (Hawkins, 1967a; 1967b). Possible Ba uptake by clinoptilolite was noted in the Thomas Range tuff (Lindsey, 1975), but Ba concentration is controlled principally by detrital processes in the tuff at Keg Mountain. As was the case for the Thomas Range tuff, the advanced stage of diagenesis of water-laid tuff at Keg Mountain is marked by feldspathization with little relative change in chemical composition.

MINERALIZATION

No evidence for mineralization in the Keg Mountain area was found by study of the mineralogy and trace element content of the water-laid tuff. Little fluorite was found, and the occurrences of argillic tuff do not contain unusual concentrations of trace elements known to be associated with beryllium or other mineralization. The frequency distribution for Be is nearly symmetrical, in contrast to the highly skewed frequency distribution for Be in the tuff of the Thomas Range (Lindsey, 1975). No regional concentrations of beryllium in tuff were discerned by trend surface analysis. The association of Pb-Ga-Be, discovered by *R*-mode factor analysis of data on the Keg Mountain tuff, probably reflects concentration in the silicic, vapor-rich parent magma.

REFERENCES CITED

Chayes, Felix, 1960, On correlation between variables of a constant sum: Jour. Geophys. Research, v. 65, no. 12, p. 4185–4193.

Cohenour, R. E., 1963, The beryllium belt of western Utah, *in* Beryllium and uranium mineralization in western Juab County, Utah: Utah Geol. Soc. Guidebook to the Geology of Utah, no. 17, p. 4–7.

Connor, J. J., Feder, G. L., Erdman, J. A., and Tidball, R. R., 1972, Environmental geochemistry in Missouri—A multidisciplinary study *in* Earth Sciences and the Quality of Life: Internat. Geol. Cong., 24th, Montreal, Canada, 1972, Symposium 1, p. 7–14.

Cooley, W. W., and Lohnes, P. R., 1962, Multivariate procedures for the behavioral sciences: New York, Wiley, 211 p.

Deer, W. A., Howie, R. A., and Zussman, J., 1962, Rock-forming minerals: London, Longmans, Green asnd Co. Ltd., 5 v.

Erickson, M. P., 1963, Volcanic geology of western Juab County, Utah, *in* Beryllium and uranium mineralization in western Juab County, Utah: Utah Geol. Soc. Guidebook to the Geology of Utah, no. 17, p. 23–35.

Freund, J. E., 1960, Modern elementary statistics [2d ed.]: Englewood Cliffs, N. J., Prentice-Hall, 413 p.

Harman, H. H., 1960, Modern factor analysis [2d ed., revised] Chicago: Univ. Chicago Press, 471 p.

Havens, R. G., and Myers, A. T., 1973, Direct-reader spectrometric analyses, *in* Vine, J. D., and Tourtelot, E. B., Geochemistry of lower Eocene sandstones in the Rocky Mountain region: U. S. Geol. Survey Prof. Paper 789, p. 13–14.

Hawkins, D. B., 1967a, Zeolites studies—[Pt.] 1, Synthesis of some alkaline earth zeolites: Materials Research Bull., v. 2, no. 10, p. 951–958.

———1967b, Zeolites studies—[Pt.]2, Ion-exchange properties of some synthetic zeolites: Materials Research Bull., v. 2, no. 11, p. 1021–1028

Hay, R. L., 1963, Stratigraphy and zeolitic diagenesis of the John Day Formation of Oregon: California Univ. Pubs. Geol. Sci., v. 42, no. 5, p. 199–262.

Howarth, R. J., 1967, Trend-surface fitting to random data—An experimental test: Am. Jour. Sci. v. 265, no. 7, p. 619–625.

Klug, H. P., and Alexander, L. E., 1954, X-ray diffraction procedures—for polycrystalline and amorphous materials: New York, John Wiley and Sons, 716 p.

Krumbein, W. C., and Graybill, F. A., 1965, An introduction to statistical models in geology: New York, McGraw-Hill Book Co., 475 p.

Lindsey, D. A., 1975, Mineralization halos and diagenesis in water-laid tuff of the Thomas Range, Utah: U. S. Geol. Survey Prof. Paper 818-B (in press).

Lindsey, D. A., Buzard, K. A., Conklin, N. M., and Lee, L. M., 1974, Mineralogical and trace element data for water-laid tuff at Keg Mountain, Juab County, Utah: U. S. Geol. Survey Rept. USGS-GD-74-012, 30 p.; available only from U. S. Dept. Commerce Natl. Tech. Inf. Service, Springfield, Va. 22161, as Rept. PB-231925.

Lindsey, D. A., Ganow, Harold, and Mountjoy, Wayne, 1973, Hydrothermal alteration associated with beryllium deposits at Spor Mountain, Utah: U. S. Geol. Survey Prof. Paper 818-A, 20 p.

Miesch, A. T., 1967a, Methods of computation for estimating geochemical abundance: U. S. Geol. Survey Prof. Paper 574-B, 15 p.

———1967b, Theory of error in geochemical data: U. S. Geol. Survey Prof. Paper 574-A, 17 p.

———1969, The constant sum problem in geochemistry, *in* Merriam, D. F., ed., Computer applications in the earth sciences—Conf., Kansas Univ., 1969, Proc.: New York, Plenum Press, p. 161-176.

Miesch, A. T., Chao, E. C. T., and Cuttitta, Frank, 1966, Multivariate analysis of geochemical data on tektites: Jour. Geology, v. 74, no. 5, pt. 2, p. 673-691.

Schultz, L. G., 1964, Quantitative interpretation of mineralogical composition from X-ray and chemical data for the Pierre Shale: U. S. Geol. Survey Prof. Paper 391-C, 31 p.

Shawe, D. R., 1966, Arizona-New Mexico and Nevada-Utah beryllium belts, *in* Geological Survey research: U. S. Geol. Survey Prof. Paper 550-C, p. C206-C213.

———1968, Geology of the Spor Mountain beryllium district, Utah, *in* Ridge, J. D., ed., Ore deposits of the United States, 1933-1967 (Graton-Sales Volume): Am. Inst. Mining, Metall. and Petroleum Engineers, v. 2, pt. 8, chap. 55, p. 1148-1161.

———1972, Reconnaissance geology and mineral potential of Thomas, Keg, and Desert calderas, central Juab County, Utah, *in* Geological Survey research 1972: U. S. Geol. Survey Prof. Paper 800-B, p. B67-B77.

Staatz, M. H., and Carr, W. J., 1964, Geology and mineral deposits of the Thomas and Dugway Ranges, Juab and Tooele Counties, Utah: U. S. Geol. Survey Prof. Paper 415, 188 p.

Staatz, M. H., and Griffitts, W. R., 1961, Beryllium-bearing tuff in the Thomas Range, Juab County, Utah: Econ. Geology, v. 56, no. 5, p. 941-950.

Tatlock, D. B., 1966, Rapid modal analysis of some felsic rocks from calibrated X-ray diffraction patterns: U. S. Geol. Survey Bull. 1209, 41 p.

☆U.S. GOVERNMENT PRINTING OFFICE: 1975—677-311/54